APP homologs, and one can reconstitute pure human γ-secretase in yeast and estimate the activity. Using this system, we compared the activity of PS1 and PS2 in γ-secretase complexes. Our data suggested that PS1-containing microsomes had much higher activity than PS2-containing microsomes. However, detailed analysis regarding the "active" γ-secretase complex revealed that the PS1 and PS2 complex produced similar levels of Aβ.

MATERIALS AND METHODS

Construction of γ-Secretase and Substrates—To reconstitute γ-secretase in yeast, human PS1 or PS2, NCT, Aph1a-L-HA, FLAG-Pen2, and substrates were cloned into the following vectors, as described previously (15). Briefly, PS1 or PS2 and NCT were ligated into KpnI and XbaI sites of the pBEVY-T vector (16). Aph1a-L-HA and FLAG-Pen2 were ligated into the XbaI and KpnI sites of pBEVY-L (16). C55-Gal4p, NotchTM-Gal4p, and C99 were fused to the *SUC2* signal sequence, facilitating translocation to the endoplasmic reticulum, and ligated into the BamHI and EcoRI sites of p426ADH (17). C55, C99, and NotchTM indicate amino acids 672–726 of the human APP770 isoform, 672–770 of the human APP770, 1703–1754 of the mouse Notch-1, respectively.

Myc-tagged PS1 and PS2 were PCR amplified and ligated into the KpnI site of pBEVY-T, using the following two pair of primers, respectively: mycPS1S, 5′-GGGGTACCAAAAA-TGGAACAAAAACTCATCTCAGAAGAGGATCTGATGA-CAGAGTTACCTGCACCGTTG-3′ and PS1AS, 5′-GATC-CGCTTATTTAGAAGTGTCGAATTCGACCTCGGTACC-ATGCTAGATATAAAATTGATGGAATGC-3′; mycPS2S, 5′-GGGGTACCAAAAATGGAACAAAAACTCATCTCAG-AAGAGGATCTGATGCTCACATTCATGGCCTCTGAC-3′ and PS2AS, 5′-GGGGTACCTCAGATGTAGAGCTGA-TGGGAGG-3′.

Yeast Transformation—Three plasmids were transformed into *Saccharomyces cerevisiae* strain PJ69–4A (*MATa, trp1–901, leu2–3, 112, ura3–52, his3–200, gal4Δ, gal80Δ, LYS2::GAL1-HIS3, GAL2-ADE2, met2::GAL7-lacZ*) (18). The transformants were selected on SD media plate lacking Leu, Trp, and Ura (SD-LWU). In microsome assays, we used the yeast strain PJ69–4Apep4Δ(*MATa, trp1–901, leu2–3, 112, ura3–52, his3–200, gal4Δ, gal80Δ, LYS2::-GAL1-HIS3, GAL2-ADE2, met2::GAL7-lacZ, pep4::kanMX*) (14) to avoid endogenous protease activity.

Reporter Gene Expression—Expression of *HIS3* (His) and *ADE2* (Ade) was estimated by transformant growth on SD-LWHUAde. β-Galactosidase assays were performed as described previously (15). Transformants were cultured in SD-LWU media until they reached an A_{600} of ~0.8. Cells were collected after centrifugation and suspended in lysis buffer (20 mM Tris-Cl (pH 8.0), 10 mM $MgCl_2$, 50 mM KCl, 1 mM EDTA, 5% glycerol, 1 mM dithiothreitol) including protease inhibitor mixture (Sigma), and lysed by glass beads. Protein concentration and β-galactosidase activity of the cell lysates were determined.

γ-Secretase Assay and Immunoblotting—Using yeast microsomes, we detected Aβ using an in vitro γ-secretase assay. *In vitro* γ-secretase assays were performed as described previously, with minor modifications (14). Microsomes (80 μg) were solubilized with γ-buffer (50 mM MES (pH 5.5) or 50 mM PIPES (pH 6.0, 6.5, 7.0, 7.5), or 50 mM HEPES (pH 8.0), 250 mM sucrose, 1 mM EGTA) containing 1% CHAPSO on ice for 60 min. Inhibitor mixture, thiorphan, *O*-phenanthroline, CHAPSO, and γ-buffer were added to the solubilized microsomes, as described previously (14). The mixture was incubated at 37 °C for 0 or 24 h. After incubation, the sample was extracted with chloroform/methanol (2:1) followed by addition of sample buffer, and boiled at 100 °C for 5 min. Aβ production was analyzed by Western blotting using the specific antibody, 82E1. Band signal was quantified using an LAS-3000 luminescent image analyzer (FujiFilm, Tokyo, Japan).

Immunoprecipitation of γ-Secretase—Microsomes (400 μg) were solubilized with IP buffer containing 1% CHAPSO and protease inhibitor mixture, on ice, for 60 min. Solubilized membranes were added to 40 μl of anti-FLAG affinity gel (50% slurry) (Sigma) and rotated at 4 °C for 2 h. Beads were washed with IP buffer and suspended in sample buffer containing 8 M urea to prepare the "IP sample" from 400 μg of microsomes. The "input sample" was prepared as follows: 100 μl of sample buffer containing 8 M urea was added to 80 μg of microsomes and incubated at 65 °C for 10 min. Microsomes (8 μg, 10–11 μl) were loaded as input.

Antibodies—The following antibodies were used for immunoblotting: monoclonal antibodies against Aβ, 82E1 (IBL, Fujioka, Japan), HA (12CA5; Sigma), FLAG (M2; Sigma), and polyclonal antibodies against NCT (AB5890; Chemicon, Temecula, CA), Myc, 2272 (Cell Signaling Technology, Beverly, MA), the PS1 loop region (G1L3) (19), and the PS2 loop region (G2L) (20).

RESULTS

PS2 Was Less Active than PS1 in Growth and β-Galactosidase Assays—We constructed recombinant plasmids for γ-secretase and APP-based (C55-Gal4p) or Notch-based substrates (NotchTM-Gal4p) (15). We introduced the vectors into yeast strain PJ69, which expresses *HIS3*, *ADE2*, and *lacZ* under Gal4p control, and generated yeast transformants expressing the γ-secretase subunits (PS1 or PS2, NCT, Aph1a-L-HA, FLAG-Pen2) and an artificial substrate (C55-Gal4p or NotchTM-Gal4p). Gal4p released from C55-Gal4p or NotchTM-Gal4p by reconstituted γ-secretase activates *HIS3* and *ADE2* genes transcription. Therefore, γ-secretase activity was assessed by growth on media lacking histidine and adenine. As a result, yeast expressing PS1 γ-secretase and C55-Gal4p could replicate on the selection media. Yeast expressing PS2 γ-secretase could also grow, but was much slower than that of PS1-expressing yeast (Fig. 1*A*). PS1 L166P, G384A, and PS2 N141I are familial Alzheimer disease (FAD) mutations. Yeast carrying these mutations were unable to grow on media lacking histidine and adenine. After isolating these yeast cell lysates, we measured β-galactosidase activity to estimate γ-secretase activity. PS1 had ~24 times more β-galactosidase activity than PS2 (Fig. 1*B*). The results of the β-galactosidase assay were well correlated with the growth assay results (Fig. 1, *A* and *B*).

Next, we used NotchTM-Gal4p as a substrate instead of C55-Gal4p. The results were similar to those obtained when using

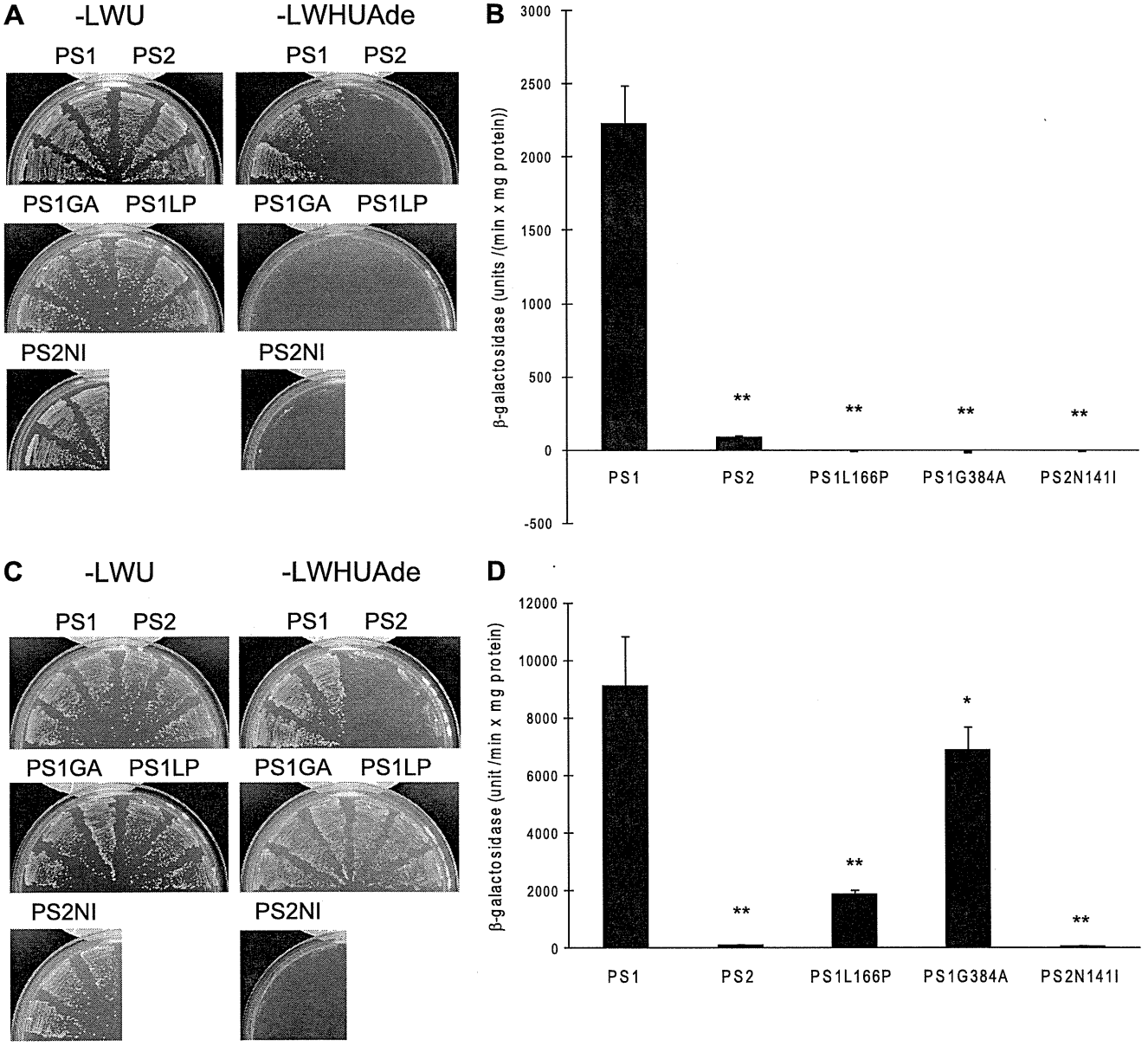

FIGURE 1. **Estimate of reconstituted PS1 or PS2 γ-secretase activity in yeast.** *A* and *C*, yeast cells were transformed with PSs (PS1 or PS2, or PS with FAD mutations), NCT, FLAG-Pen2, Aph1a-L-HA, and C55-gal4p (*A*), or NotchTM-gal4p (*C*). Three independent clones were cultured on non-selection media (SD-LWU) or selection media (SD-LWHUAde) at 30 °C for 3 days. Yeast cells not expressing PS did not grow on SD-LWHUAde. *B* and *D*, β-galactosidase activity was measured for each yeast lysate. Lysates were prepared from yeast cells using glass beads. One unit of β-galactosidase activity corresponds to 1 nmol of *O*-nitrophenyl β-d-galactopyranoside hydrolyzed per min, and activity was calculated as unit/(min × mg of protein in lysate). The activity was normalized by subtracting the activity in the absence of PS, 65 unit/(min × mg protein). Data are presented as mean value ± S.D., $n = 18$ (*A*), $n = 3$ (*C*) *, $p < 0.05$; **, $p < 0.01$ (analyzed by one-way analysis of variance followed by Dunnett's multiple comparison test). Statistical analyses were performed with PRISM software.

the C55-Gal4p, with the following two exceptions. Notch1 was more likely to be cleaved by γ-secretase than C55 (APP) (Fig. 1, *B versus D*) and yeast cells expressing PS1 with FAD mutations (L166P and G384A) were able to grow on SD-LWHUAde, whereas cells expressing PS2 N141I were not (Fig. 1*D*). These results suggested that PS1 with the FAD mutations cannot cleave APP, whereas they can cleave Notch like wild-type γ-secretase.

Optimal pH for Aβ Production by the PS2 Complex—To study γ-secretase activity *in vitro*, we prepared yeast microsomes from yeast transformants expressing PS1 or PS2, NCT, Aph1a-L-HA, FLAG-Pen2, and C55 (14). Three previous reports showed that γ-secretase with PS1 maximally produced Aβ at approximately pH 7.0 (14, 21, 22). The optimum pH of Aβ production by γ-secretase with PS2, however, remains unclear. Thus, we investigated the optimal pH of the PS2 complex to produce Aβ. When yeast microsomes prepared from three independent clones were incubated for 24 h at 37 °C with 0.25% CHAPSO and 0.1% PC, we found that the PS2 complex also maximally produced Aβ at approximately pH 7.0 in all three assays (Fig. 2, *A* and *B*), suggesting that the PS1 and PS2 complex have similar pH dependences for Aβ production.

Levels of Aβ Production by PS1 or PS2—We compared the level of Aβ produced by PS1 or PS2 using yeast microsomes. Each microsome was incubated at 37 °C for 24 h in the pres-

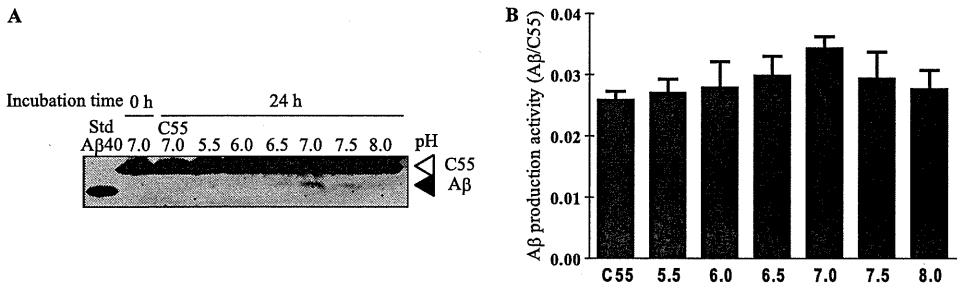

FIGURE 2. **Optimum pH of Aβ production by PS2.** *A*, microsomes (80 μg) prepared from three independent yeast cells transformed with PS2, NCT, Aph1a-L-HA, FLAG-Pen2, and C55, and from yeast expressing C55 were incubated with 0.25% CHAPSO and 0.1% PC at 37 °C for 0 or 24 h. Incubation samples were subjected to immunoblotting to compare Aβ production activity, Aβ/C55. Aβ was detected by 82E1. Synthetic Aβ40 (20 pg) was used as a positive control. Yeast expressing C55 and microsomes incubated for 0 h were loaded as a negative control. *B*, three independent assays were quantified using analyzing software (LAS-3000 luminescent image analyzer, Fuji Film, Tokyo, Japan). The column represents the mean ± S.D. ($n = 3$).

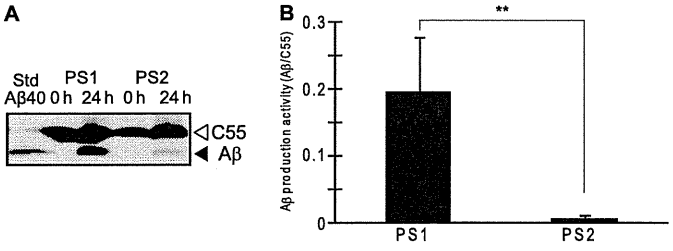

FIGURE 3. **Difference in Aβ production between PS1 and PS2.** *A*, yeast microsomes expressing PS1 or PS2, NCT, Aph1a-L-HA, FLAG-Pen2, and C55 were subjected to *in vitro* γ-secretase assays at pH 7.0. Aβ produced by PS1 or PS2 γ-secretase was detected. Synthetic Aβ40 (30 pg) was loaded as a marker. *B*, the bands obtained in *A* were quantified to determine the ratio of Aβ to C55 using analyzing software (LAS-3000 luminescent image analyzer, Fuji Film, Tokyo, Japan). The column represents the mean ± S.D. ($n = 5$, **, $p < 0.01$). Data were analyzed by Student's *t* test.

ence of 0.25% CHAPSO and 0.1% PC. We found that the PS1 complex produced significantly more Aβ than PS2 (Fig. 3*A*). By quantifying the Western blotting signals, we calculated that PS1 produced ~24 times more Aβ than PS2 (Fig. 3*B*).

PS1 Complexes Were More Abundant than PS2 Complexes—To verify whether PS, NCT, Aph1a-L, and Pen2 form the γ-secretase complex, we isolated membrane fractions from yeast introduced with PS, NCT, Aph1a-L-HA, FLAG-Pen2, and C99, and performed co-immunoprecipitation experiments with the anti-FLAG M2 affinity gel. Both PS1 and PS2 were co-immunoprecipitated with FLAG-Pen2 (Fig. 4, *B* and *C*). NCT and Aph1a-L were also co-immunoprecipitated with FLAG-Pen2 (Fig. 4*A*), suggesting that PS1 and PS2 formed a γ-secretase complex. We also found that the PS2 complex predominantly included non-glycosylated immature NCT, whereas the PS1 complex contained highly glycosylated mature NCT (Fig. 4*A*).

Comparison of the PS1 and PS2 contents in γ-secretase is difficult due to the variable affinity of their specific antibodies. To estimate the amount of PS1 or PS2 in γ-secretase complexes, we constructed Myc-tagged PS1 and PS2. We introduced these constructs into yeast and reconstituted the γ-secretases. Preparing these microsomes, we immunoprecipitated γ-secretase complexes with anti-FLAG affinity gel. The immunoprecipitates were next subjected to immunoblotting. Aph1a-L levels in the PS1 or PS2 complex were similar (Fig. 5*A*). The Myc-tagged PS1 complex included mainly mature NCT, while Myc-tagged PS2 complexes contained immature NCT (Fig. 5*A*). The level of PS1 NTF in γ-secretase complexes (associated with FLAG Pen2) was ~28 times higher than that of PS2 NTF (Fig. 5*B*).

When calculating γ-secretase activity per one γ-secretase complex from these data, a significant difference between PS1 and PS2 does not exist. However, the PS1 complex was 24.15 more active in the β-galactosidase assay. *In vitro* Aβ production assays indicated that PS1 was 24.61 more active than PS2. Comparing PS1 and PS2 contents in γ-secretase in a co-immunoprecipitation experiment, we found that the amount of PS1NTF in the γ-secretase complex was 28.14 times higher than that of PS2NTF. These data suggested that the complete PS2 complex was 1.142 or 1.143 times more active than the PS1 complex.

DISCUSSION

γ-Secretase assays measuring released Aβ into conditioned media from cultured cells have been previously performed. These assays found that γ-secretase with PS FAD mutations increased the Aβ 40/42 ratio. However, very few *in vitro* assays have been reported. To accurately study γ-secretase activity, Yagishita *et al.* (14) established an *in vitro* assay system using yeast, which possesses no γ-secretase homologs. This system enabled us to directly compare activities between the PS1 and PS2 complex.

Yeast growth and β-galactosidase assays using C55-Gal4p or Notch-Gal4p as a substrate revealed that PS1 had a significantly higher activity than PS2. We also found that FAD mutations in PS abolished APP processing activity, and that PS1 L166P and G384A cleaved Notch with reduced activity compared with wild-type PS1. The assembly of PS1 FAD mutants (L166P or G384A) into γ-secretase complex was also assessed by immunoprecipitation (supplemental Fig. S1). The assembly of PS1 L166P mutant was similar to PS1 WT. On the other hand, ~36% of PS1 G384A (comparing to the WT) formed the γ-secretase complex. These results showed that PS1 L166P assembled normally with defective protease activity and PS1 G384A was defective both in the assembly and the protease activity, suggesting that loss of function of PS caused lower cleavage activity. These reductions in processing activity obtained in this report support PS loss of function hypothesis, which is believed to cause FAD (23). We evaluated the activity of other PS1 FAD mutations (A79V, M146L, A231V, M233T, and ΔExon9) in Notch cleavage (data not shown). Our Notch

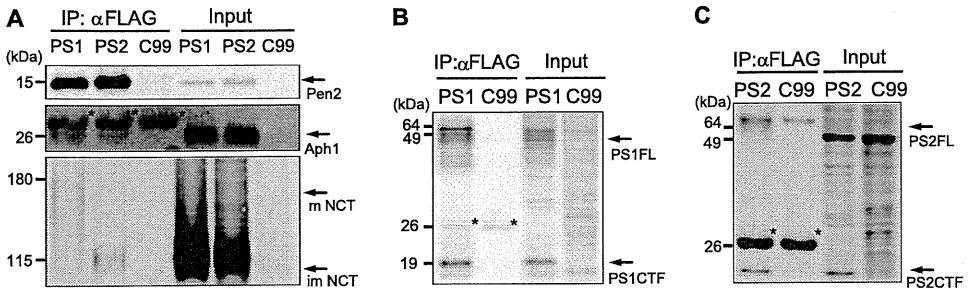

FIGURE 4. **Formation of PS1 and PS2 γ-secretase complexes.** Yeast microsomes expressing PS1 or PS2, NCT, Aph1a-L-HA, FLAG-Pen2, and C99, and microsomes expressing C99 were solubilized with IP buffer containing 1% CHAPSO and protease inhibitor mixture. γ-Secretase complexes were immunoprecipitated with anti-FLAG affinity gel (Sigma). The immunoprecipitates and input fraction were subjected to immunoblotting. NCT, Aph1, Pen2, and PS were detected by specific antibodies. The *asterisks* indicate nonspecific bands.

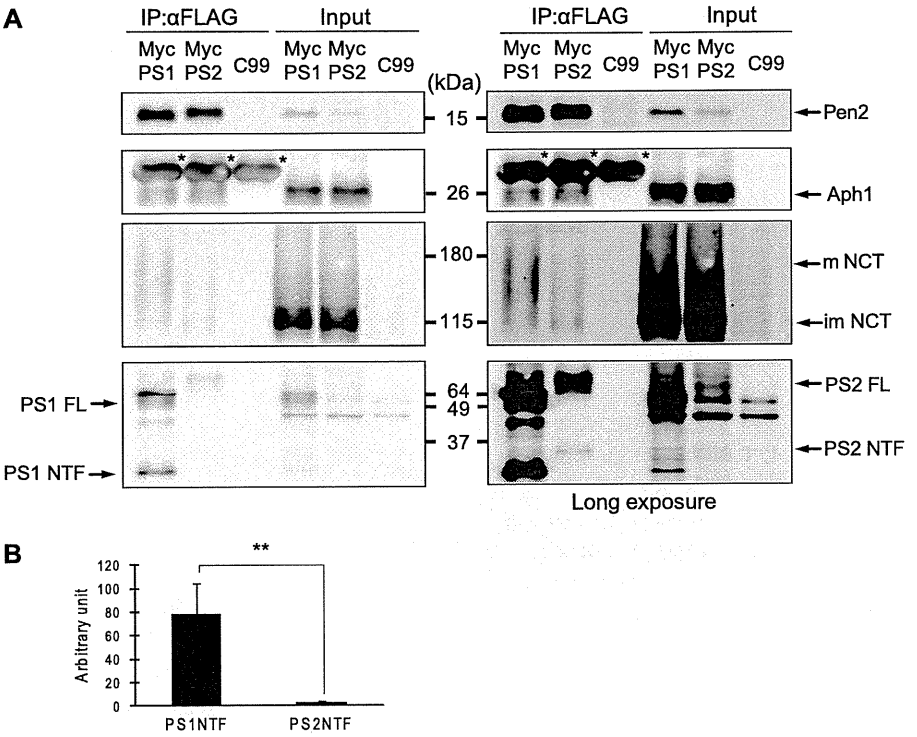

FIGURE 5. **Quantification of PS1 and PS2 in γ-secretase complexes.** *A*, yeast expressing Myc-tagged PS1 or PS2, the other secretase subunits, and C99, were incubated with anti-FLAG affinity gel. The immunoprecipitates were analyzed by immunoblotting. *B*, amount of Myc-tagged PS1NTF and Myc-tagged PS2NTF in the γ-secretase complexes were quantified using LAS-3000 luminescent image analyzer (Fuji Film, Tokyo, Japan). Data were analyzed by Student's *t* test. Error bar shows the mean ± S.D. $n = 4$, **, $p < 0.01$. The *asterisks* indicate nonspecific bands.

cleavage results with PS1 FAD mutations, PS1L166P and G384A, corroborated the findings of earlier studies (24, 25).

Based on the *in vitro* γ-secretase assay using yeast microsomes, we found that γ-secretase with PS2 optimally produced Aβ at approximately pH 7.0. Previous reports have shown that PS1 also maximally produced Aβ at pH 7.0 (14, 21, 22), suggesting that PS1 and PS2 make Aβ using a similar mechanism.

Our co-immunoprecipitation experiments using yeast microsomes containing PS1 or PS2, NCT, Aph1a-L-HA, and FLAG-Pen2 showed that PS2 bound to immature NCT, whereas PS1 bound to the mature NCT. Expression levels of immature or mature NCTs in cells transformed with PS1 or PS2 were similar, but the anti-FLAG affinity gel immunoprecipitates contained different levels of immature and mature NCT. Frånberg *et al.* (26) reported that Ps2 bound to immature NCT in Ps1-deficient (Ps1-(−/−), Ps2-(+/+)) MEF cells and Ps1 bound to mature NCT in Ps2 deficient (Ps1-(+/+), Ps2-(−/−)) MEF cells using affinity capture with an active site-directed γ-secretase inhibitor. This difference in NCT maturation in the complex may affect substrate affinity.

In this study, we used Aph1a-L as a γ-secretase subunit, which may facilitate PS2 binding to immature NCT. Also, Aph1a-S expression, or Aph1b as a γ-secretase subunit, may result in alternative binding patterns, such as PS2 binding to mature NCT or PS1 binding with immature NCT. In fact, we observed the PS1 complex with Aph1a-S containing more immature NCT than the PS1 complex with Aph1a-L (data not shown). To date, γ-secretase is known to target many substrates, but how γ-secretase selects its substrates is unclear. These variable γ-secretases may contribute to specific substrate selection.

To compare the γ-secretase activity of PS1 and PS2 precisely, we employed two different approaches. First, we used C55(-Gal4p) or C99 as a substrate instead of C100Flag. NCT

plays a role in binding to the substrate by recognizing N terminus of C99 (27). So, natural N terminus of C99 or C55 is important to assess γ-secretase activity correctly. Using C100Flag as a substrate may result in inaccurate evaluation, because C100Flag possesses one extra amino acid, methionine, on the N terminus. Second, we estimated the amount of PS1 or PS2 in the γ-secretase complex. Lai *et al.* (13) reported Ps1 and Ps2 γ-secretase activity as a function of total protein concentration, but not all PS localizes to the γ-secretase complex. Therefore, γ-secretase activity should be calculated as follows: γ-secretase activity/concentration of PS in γ-secretase complex. γ-Secretase assembly is not a random process, but occurs sequentially. NCT and Aph1 form the NCT-Aph1 subcomplex in the initial step of complex formation. Two hypotheses have been proposed regarding the subsequent steps in γ-secretase complex assembly. One hypothesis is that PS binds to the NCT-Aph1 subcomplex, followed by Pen2, creating a γ-secretase complex (28, 29). Alternatively, the PS-Pen2 intermediate may bind to the preexisting NCT-Aph1 subcomplex to form the γ-secretase complex (30). To evaluate the construction process of the γ-secretase complex, we compared PS1 or PS2 in the γ-secretase complex by co-immunoprecipitating Myc-tagged PS1 or PS2 with anti-FLAG antibody (FLAG tag is on Pen2). Co-immunoprecipitation with other antibodies detecting NCT, Aph1, or PS could lead to inaccurate estimates regarding the amount of Myc-PS in the γ-secretase complex. We found that the concentration of PS2 in the γ-secretase complex was much lower than that of PS1. Because we applied a minimal reconstitution system in yeast, unknown protein(s) may stabilize PS2. This possibility is currently being explored.

In this study, we reconstituted human PS1 and PS2 γ-secretase complexes and compared their Aβ production (per γ-secretase complex). PS1 had 24.65 times and 24.61 times higher activity than PS2 in the β-galactosidase and *in vitro* Aβ production assay, respectively. Based on Co-IP experiments, the amount of PS1 in the γ-secretase complex was 28.14 times higher than that of PS2. Thus, our data suggest that PS1 did not have significantly higher activity than PS2, as has been reported (13). PS1 and PS2 were 67% identical at the amino acid level, suggesting that these two proteins have related functions in the γ-secretase complex. Our results suggest that the difference between PS1 and PS2 is their affinity to the other γ-secretase subunits. The contribution of PS1 on γ-secretase activity is more important than that of PS2 because PS1 knock-out mice exhibit severe phenotypes, whereas PS2 knock-out mice do not. We hypothesize that the differences in PS1 and PS2 knock-out mice phenotypes may result from different amounts of PS1 and PS2 γ-secretases, but not differences in their activity.

Currently, PS1 is believed to have a higher activity than PS2 in γ-secretases, while we showed that they have similar activities. In corroboration of our findings, recent reports have shown that PS2 γ-secretase cleaved more APP than PS1 γ-secretase in microglia cells, regardless of the presence of PS1 (31). Thus, when studying γ-secretase activity, we should consider the concentration of PS in the active γ-secretase complex, which may aid in clarifying the pathogenesis of FAD caused by PS loss-of-function FAD mutations.

Acknowledgments—We thank Dr. Raphael Kopan for the mNotch1 clone and Dr. Philip James for the PJ-69–4A yeast strain. We also thank the members of our laboratory, especially Yusuke Nagara, Natsumi Ohsawa, and Yuri Watanabe for helpful discussions and technical suggestions.

REFERENCES

1. Edbauer, D., Winkler, E., Regula, J. T., Pesold, B., Steiner, H., and Haass, C. (2003) *Nat. Cell Biol.* **5,** 486–488
2. Wolfe, M. S., Xia, W., Ostaszewski, B. L., Diehl, T. S., Kimberly, W. T., and Selkoe, D. J. (1999) *Nature* **398,** 513–517
3. Steiner, H., Duff, K., Capell, A., Romig, H., Grim, M. G., Lincoln, S., Hardy, J., Yu, X., Picciano, M., Fechteler, K., Citron, M., Kopan, R., Pesold, B., Keck, S., Baader, M., Tomita, T., Iwatsubo, T., Baumeister, R., and Haass, C. (1999) *J. Biol. Chem.* **274,** 28669–28673
4. Jarrett, J. T., and Lansbury, P. T., Jr. (1993) *Cell* **73,** 1055–1058
5. Sato, T., Diehl, T. S., Narayanan, S., Funamoto, S., Ihara, Y., De Strooper, B., Steiner, H., Haass, C., and Wolfe, M. S. (2007) *J. Biol. Chem.* **282,** 33985–33993
6. Shirotani, K., Tomioka, M., Kremmer, E., Haass, C., and Steiner, H. (2007) *Neurobiol. Dis.* **27,** 102–107
7. Lee, M. K., Slunt, H. H., Martin, L. J., Thinakaran, G., Kim, G., Gandy, S. E., Seeger, M., Koo, E., Price, D. L., and Sisodia, S. S. (1996) *J. Neurosci.* **16,** 7513–7525
8. Zhang, J., Kang, D. E., Xia, W., Okochi, M., Mori, H., Selkoe, D. J., and Koo, E. H. (1998) *J. Biol. Chem.* **273,** 12436–12442
9. Levitan, D., Doyle, T. G., Brousseau, D., Lee, M. K., Thinakaran, G., Slunt, H. H., Sisodia, S. S., and Greenwald, I. (1996) *Proc. Natl. Acad. Sci. U.S.A.* **93,** 14940–14944
10. Shen, J., Bronson, R. T., Chen, D. F., Xia, W., Selkoe, D. J., and Tonegawa, S. (1997) *Cell* **89,** 629–639
11. Wong, P. C., Zheng, H., Chen, H., Becher, M. W., Sirinathsinghji, D. J., Trumbauer, M. E., Chen, H. Y., Price, D. L., Van der Ploeg, L. H., and Sisodia, S. S. (1997) *Nature* **387,** 288–292
12. Herreman, A., Hartmann, D., Annaert, W., Saftig, P., Craessaerts, K., Serneels, L., Umans, L., Schrijvers, V., Checler, F., Vanderstichele, H., Baekelandt, V., Dressel, R., Cupers, P., Huylebroeck, D., Zwijsen, A., Van Leuven, F., and De Strooper, B. (1999) *Proc. Natl. Acad. Sci. U.S.A.* **96,** 11872–11877
13. Lai, M. T., Chen, E., Crouthamel, M. C., DiMuzio-Mower, J., Xu, M., Huang, Q., Price, E., Register, R. B., Shi, X. P., Donoviel, D. B., Bernstein, A., Hazuda, D., Gardell, S. J., and Li, Y. M. (2003) *J. Biol. Chem.* **278,** 22475–22481
14. Yagishita, S., Futai, E., and Ishiura, S. (2008) *Biochem. Biophys. Res. Commun.* **377,** 141–145
15. Futai, E., Yagishita, S., and Ishiura, S. (2009) *J. Biol. Chem.* **284,** 13013–13022
16. Miller, C. A., 3rd, Martinat, M. A., and Hyman, L. E. (1998) *Nucleic Acids Res.* **26,** 3577–3583
17. Mumberg, D., Müller, R., and Funk, M. (1995) *Gene* **156,** 119–122
18. James, P., Halladay, J., and Craig, E. A. (1996) *Genetics* **144,** 1425–1436
19. Tomita, T., Takikawa, R., Koyama, A., Morohashi, Y., Takasugi, N., Saido, T. C., Maruyama, K., and Iwatsubo, T. (1999) *J. Neurosci.* **19,** 10627–10634
20. Tomita, T., Tokuhiro, S., Hashimoto, T., Aiba, K., Saido, T. C., Maruyama, K., and Iwatsubo, T. (1998) *J. Biol. Chem.* **273,** 21153–21160
21. Li, Y. M., Lai, M. T., Xu, M., Huang, Q., DiMuzio-Mower, J., Sardana, M. K., Shi, X. P., Yin, K. C., Shafer, J. A., and Gardell, S. J. (2000) *Proc. Natl. Acad. Sci. U.S.A.* **97,** 6138–6143
22. Fraering, P. C., Ye, W., Strub, J. M., Dolios, G., LaVoie, M. J., Ostaszewski, B. L., van Dorsselaer, A., Wang, R., Selkoe, D. J., and Wolfe, M. S. (2004) *Biochemistry* **43,** 9774–9789
23. Shen, J., and Kelleher, R. J., 3rd (2007) *Proc. Natl. Acad. Sci. U.S.A.* **104,** 403–409
24. Steiner, H., Kostka, M., Romig, H., Basset, G., Pesold, B., Hardy, J., Capell, A., Meyn, L., Grim, M. L., Baumeister, R., Fechteler, K., and Haass, C.

(2000) *Nat. Cell Biol.* **2,** 848–851
25. Moehlmann, T., Winkler, E., Xia, X., Edbauer, D., Murrell, J., Capell, A., Kaether, C., Zheng, H., Ghetti, B., Haass, C., and Steiner, H. (2002) *Proc. Natl. Acad. Sci. U.S.A.* **99,** 8025–8030
26. Frånberg, J., Svensson, A. I., Winblad, B., Karlström, H., and Frykman, S. (2011) *Biochem. Biophys. Res. Commun.* **404,** 564–568
27. Shah, S., Lee, S. F., Tabuchi, K., Hao, Y. H., Yu, C., LaPlant, Q., Ball, H., Dann, C. E., 3rd, Südhof, T., and Yu, G. (2005) *Cell* **122,** 435–447
28. LaVoie, M. J., Fraering, P. C., Ostaszewski, B. L., Ye, W., Kimberly, W. T., Wolfe, M. S., and Selkoe, D. J. (2003) *J. Biol. Chem.* **278,** 37213–37222
29. Niimura, M., Isoo, N., Takasugi, N., Tsuruoka, M., Ui-Tei, K., Saigo, K., Morohashi, Y., Tomita, T., and Iwatsubo, T. (2005) *J. Biol. Chem.* **280,** 12967–12975
30. Fraering, P. C., LaVoie, M. J., Ye, W., Ostaszewski, B. L., Kimberly, W. T., Selkoe, D. J., and Wolfe, M. S. (2004) *Biochemistry* **43,** 323–333
31. Jayadev, S., Case, A., Eastman, A. J., Nguyen, H., Pollak, J., Wiley, J. C., Möller, T., Morrison, R. S., and Garden, G. A. (2010) *PloS One* **5,** e15743

Biochemical and Biophysical Research Communications 417 (2012) 462–467

Contents lists available at SciVerse ScienceDirect

Biochemical and Biophysical Research Communications

journal homepage: www.elsevier.com/locate/ybbrc

Tumor suppressor cell adhesion molecule 1 (CADM1) is cleaved by a disintegrin and metalloprotease 10 (ADAM10) and subsequently cleaved by γ-secretase complex

Yusuke Nagara [a], Man Hagiyama [b,c], Naoya Hatano [d], Eugene Futai [a,1], Satoshi Suo [a], Yutaka Takaoka [e], Yoshinori Murakami [b], Akihiko Ito [b,c,*], Shoichi Ishiura [a]

[a] Department of Life Sciences, Graduate School of Arts and Sciences, The University of Tokyo, 3-8-1 Komaba, Meguro-ku, Tokyo 153-8902, Japan
[b] The Division of Molecular Pathology, Institute of Medical Science, The University of Tokyo, 4-6-1 Shirokanedai, Minato-ku, Tokyo 108-8639, Japan
[c] Department of Pathology, Faculty of Medicine, Kinki University, 377-2 Ohno-Higashi, Osaka-Sayama, Osaka 589-8511, Japan
[d] The Integrated Center for Mass Spectrometry, Kobe University Graduate School of Medicine, 7-5-1 Kusunoki-cho, Chuo-ku, Kobe 650-0017, Japan
[e] Division of Medical Informatics and Bioinformatics, Kobe University Hospital, 7-5-2 Kusunoki-cho, Chuo-ku, Kobe 650-0017, Japan

ARTICLE INFO

Article history:
Received 21 November 2011
Available online 7 December 2011

Keywords:
CADM1
ADAM10
γ-Secretase
Shedding
RIP
Tumor suppressor gene

ABSTRACT

Cell adhesion molecule 1 (CADM1) is a type I transmembrane glycoprotein expressed in various tissues. CADM1 is a cell adhesion molecule with many functions, including roles in tumor suppression, apoptosis, mast cell survival, synapse formation, and spermatogenesis. CADM1 undergoes membrane-proximal cleavage called shedding, but the sheddase and mechanisms of CADM1 proteolysis have not been reported. We determined the cleavage site involved in CADM1 shedding by LC/MS/MS and showed that CADM1 shedding occurred in the membrane fraction and was inhibited by tumor necrosis factor-α protease inhibitor-1 (TAPI-1). An siRNA experiment revealed that ADAM10 mediates endogenous CADM1 shedding. In addition, the membrane-bound fragment generated by shedding was further cleaved by γ-secretase and generated CADM1-intracellular domain (ICD) in a mechanism called regulated intramembrane proteolysis (RIP). These results clarify the detailed mechanism of membrane-proximal cleavage of CADM1, suggesting the possibility of RIP-mediated CADM1 signaling.

1. Introduction

Cell adhesion molecule 1 (CADM1) is a 100–120-kDa multifunctional cell adhesion molecule. CADM1 is a member of the immunoglobulin superfamily and is a type I transmembrane glycoprotein. The extracellular domain of CADM1 undergoes homophilic or heterophilic interaction with necl-1, nectin-3, and CRTAM (class-I MHC-restricted T cell-associated molecule) [1], whereas the intracellular domain interacts with DAL-1 via its band 4.1 binding domain [2] and with pals2 [3] and MPP3 [4] via its PDZ binding domain. CADM1 is expressed in various tissues and organs, including the brain, mast cells, testis, and lung [5].

Recently, Tanabe et al. reported that CADM1 undergoes juxtamembrane cleavage in neurons [6]. We reported previously that shedding fragments were found from mast cells [7] and human mesothelioma samples [8]. These observations suggest that CADM1 shedding is a common event. CADM1 shedding seems to regulate adhesion between mesothelial and mesothelioma cells by down-regulating full-length CADM1, thereby regulating the growth and scattering of mesothelioma cells [8]. Tanabe et al. reported that certain isoforms of CADM1 produce a 20-kDa C-terminal fragment and that production of this fragment is inhibited by the broad-spectrum metalloprotease inhibitor TAPI-1. They concluded that CADM1 is shed by an ADAM17-like protease [6]. The ADAM family metalloproteases are the major membrane-bound sheddases, which are responsible for shedding of many membrane protein substrates. Among the family members, ADAM10 and ADAM17 are the major sheddases and have large numbers of known substrates. After shedding, some membrane proteins undergo a secondary cleavage within the membrane mediated by γ-secretase. For example, Notch, ErbB4, and amyloid precursor protein (APP) are cleaved by γ-secretase [9]. The γ-cleavage product, the intracellular domain (ICD) of the substrate, often acts as a transcriptional regulator. ICDs of Notch and other γ-secretase substrates, such as CD44 [10] and APP [11], act as nuclear signaling molecules that regulate gene expression.

In this study, we focused on CADM1 proteolysis. The aim of this study was to characterize the sheddase of CADM1 and to examine proteolysis events occurring on the CADM1 molecule. Our results

* Corresponding author at: Department of Pathology, Faculty of Medicine, Kinki University, 377-2 Ohno-Higashi, Osaka-Sayama, Osaka 589-8511, Japan. Fax: +81 72 360 2028.
E-mail address: aito@med.kindai.ac.jp (A. Ito).
[1] Present address: Department of Molecular Cell Science, Graduate School of Agricultural Science, Tohoku University, 1-1 Tsutsumidori Amamiya-machi, Aoba-ku, Sendai, Miyagi 981-8555, Japan.

0006-291X/$ - see front matter © 2011 Elsevier Inc. All rights reserved.
doi:10.1016/j.bbrc.2011.11.140

indicated that CADM1 shedding is catalyzed by a protease associated with the cell membrane, and ADAM10 endogenously sheds CADM1. Furthermore, we discovered γ-cleavage of CADM1, which is catalyzed by γ-secretase. These results provide a possible signal-transduction mechanism involving regulated intramembrane proteolysis (RIP).

2. Materials and methods

2.1. Reagents and antibodies

TAPI-1, *N*-[*N*-(3,5-difluorophenacetyl-L-alanyl)]-(*S*)-phenylglycine t-butyl ester (DAPT), and L-685,458 were purchased from Calbiochem (San Diego, CA). Phorbol-12-myristate-13-acetate (PMA) was purchased from Wako (Osaka, Japan). Phenylmethylsulfonyl fluoride (PMSF) and protease inhibitor cocktail (cat.# P8340) were purchased from Sigma (St. Louis, MO).

Anti-CADM1-cyto antibody was generated according to the method described by Wakayama et al. [12]. This antibody recognizes the C-terminal 20 amino acids of CADM1. Anti-CADM1-ecto antibody (3E1) is our original as described previously [13]. This antibody recognizes 2nd Ig domain in the ectodomain. Peroxidase-conjugated secondary antibodies were purchased from Cell Signaling Technology (Danvers, MA).

2.2. In vitro assay of CADM1 shedding

Confluent HEK293 cells were harvested and homogenized in buffer P (20 mM PIPES-KOH pH 7.0, 140 mM KCl, 250 mM sucrose) at 4 °C. The homogenized cells were centrifuged at 800*g* for 10 min to remove the nuclei and cell debris. The supernatant was then ultracentrifuged at 100,000*g* for 1 h, and the resulting pellet was washed with buffer P and ultracentrifuged again at 100,000*g* for 1 h. The resulting pellet (the membrane fraction) was resuspended in buffer P and stored at −80 °C until use.

This membrane fraction was incubated at 37 °C for 1.5 h with the indicated concentrations of protease inhibitors or vehicle only (DMSO, 0.2% for TAPI-1, 1% for PMSF and protease inhibitor cocktail), and the reaction was stopped by addition of 2× sample buffer and boiling for 5 min. These samples were subjected to Western blotting analysis using anti-CADM1-cyto antibody.

2.3. Western blotting analysis

SDS–PAGE and Western blotting were performed according to the standard reducing SDS–PAGE and Western blotting protocols. For detection of CADM1-ICD, samples were separated by Tris–tricine SDS–PAGE and transferred onto Immobilon-P membranes (Millipore, Billerica, MA). The membranes were boiled in PBS for 5 min after transfer and then subjected to blocking, antibody treatments, and subsequent procedures.

2.4. Transfection of siRNA and expression vectors

siRNA (Stealth Select RNAi) specific for human ADAM10 (HSS100167), ADAM17 (HSS110435), and control siRNA (Stealth RNAi negative control low GC duplex, 12935-200) were purchased from Invitrogen (Carlsbad, CA). Saos-2 cells at 40–50% confluence were transfected with siRNAs using Lipofectamine RNAiMax Transfection Reagent (Invitrogen) according to the manufacturer's instructions. After 96 h of incubation, cells were harvested, and the cell lysates were analyzed by Western blotting.

2.5. Cell culture

cDNA encoding mouse-CADM1 (GenBank ID: AB052293) was cloned into the expression vector pCX4-bsr and confirmed by DNA sequencing (pCX4bsr-CADM1) [7]. COS7 cells and NIH3T3 cells were transfected with the pCX4bsr-CADM1 vector, and blasticidin-resistant cells were selected by continuing the culture in the presence of blasticidin (3 μg/mL) for 4 weeks (COS7-mCADM1 and NIH3T3-mCADM1). MEF and nicastrin$^{-/-}$ MEF cells were kind gifts from Dr. Philip C. Wong (The Johns Hopkins University), and presenilin 1/2 double knockout MEF was a kind gift from Dr. Bart De Strooper (Vlaams Instituut voor Biotechnologie). These cells, HEK293, and human osteosarcoma Saos-2 were maintained in DMEM supplemented with 10% fetal bovine serum and penicillin/streptomycin. In γ-secretase inhibitor assay, confluent COS7-mCADM1 cells were treated with 200 ng/mL PMA for 2 h, and then γ-secretase inhibitor (1 μM DAPT or 1 μM L-685,458) or vehicle (DMSO) was added. After incubation for the indicated times, cells were harvested, and the cell lysates were analyzed by Western blotting.

2.6. Mass spectrometric analysis

NIH3T3-mCADM1 cells were harvested, and the membrane fraction extract was prepared using Subcellular Proteome Extraction Kit (Merck, Whitehouse Station, NJ). The membrane fraction extract was concentrated using Amicon Ultra 15 (Millipore) and then immunoprecipitated using anti-CADM1cyto antibody. The precipitate was mixed with sample buffer and subjected to SDS–PAGE. The gel was stained with EZ-Blue (Sigma), and the alphaCTF band was cut out. In-gel digestion with chymotrypsin was performed according to the published methods [14,15]. The digested peptides were subjected to liquid chromatography (LC)/MS/MS analysis on a Q-Tof2 quadrupole/time-of-flight (TOF) hybrid mass spectrometer (Micromass, Manchester, UK) interfaced with a capillary reversed-phase liquid chromatography system (Micromass CapLC system) as described previously [14]. The MS/MS data were analyzed with Mascot MS/MS Ion Search (version 2.1.6; Matrix Science Ltd., London, UK) to assign the obtained peptides to the NCBI non-redundant database (NCBInr 20060718; 3784285 sequences) as described previously [14].

3. Results

3.1. CADM1 shedding is promoted by phorbol ester

To study shedding of CADM1, we first generated a stable COS7 cell line expressing murine CADM1 (COS7-mCADM1). Several CADM1-derived bands, including bands of approximately 15 and 35 kDa, were detected from COS7-mCADM1 lysate by Western blotting with an antibody that recognizes the C-terminal of CADM1. We refer to the 15- and 35-kDa fragments as alphaCTF (C-terminal fragment) and betaCTF, respectively. AlphaCTF is likely to be the same shedding fragment of CADM1 reported previously [6], and betaCTF is another fragment of CADM1. As shedding of some other membrane proteins is promoted by phorbol esters such as PMA, we examined the effects of PMA treatment on CADM1 shedding (Fig. 1A) and found that alphaCTF was increased after PMA treatment. On the other hand, no apparent changes were observed in the 35-kDa band, which was thought to be another cleaved fragment of CADM1.

We next concentrated CADM1 alphaCTF by immunoprecipitation and determined the cleavage site by LC/MS/MS. Following SDS–PAGE, the gel slice containing the alphaCTF band was excised

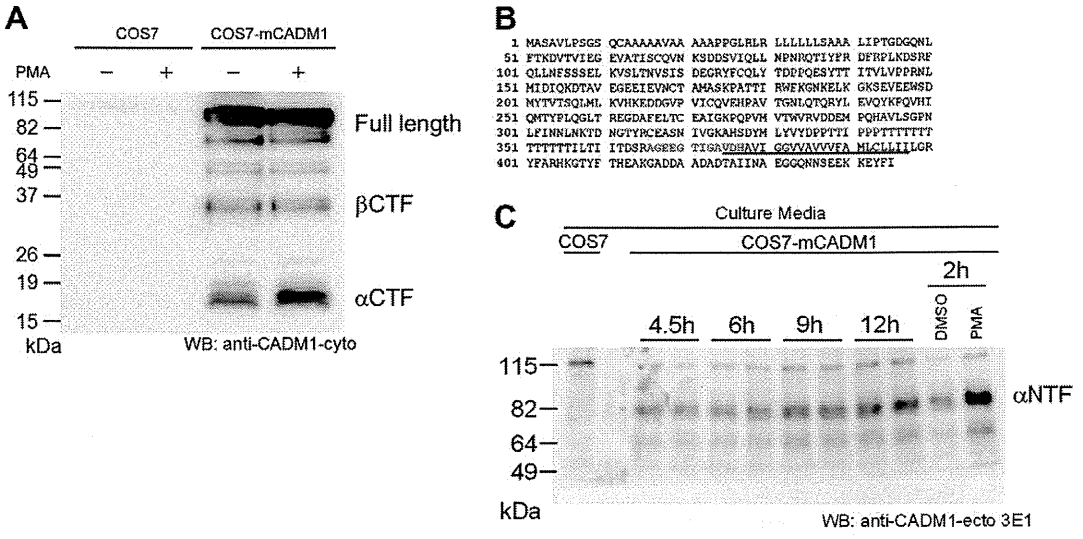

Fig. 1. Ectodomain shedding of CADM1, (A) COS7-mCADM1 cells were treated with 200 ng/mL PMA or vehicle alone for 30 min and then harvested. Cell lysates were analyzed by Western blotting using anti-CADM1-cyto antibody. (B) Determination of the cleavage site of CADM1 shedding. The peptide detected by LC/MS/MS is indicated in red, and the transmembrane region is underlined. (C) Culture medium of subconfluent COS7-mCADM1 cells was changed to serum-free medium and incubated for the indicated times (duplicate results are shown). To evaluate PMA-dependent secretion, 200 ng/mL PMA or vehicle (DMSO) was added to the serum-free medium and incubated for 2 h. The medium was then harvested and concentrated by TCA precipitation. The precipitate was analyzed by Western blotting using anti-CADM1-ecto antibody 3E1. (For interpretation of the references to color in this figure legend, the reader is referred to the web version of this article.)

and cleaved with chymotrypsin in the gel. LC/MS/MS detected a peptide fragment with an N-terminus generated by proteases other than chymotrypsin (Fig. 1B). This observation suggested that the N-terminus of the detected peptide was generated by shedding. The cleavage site was between R365 and A366, nine amino acid residues from the predicted transmembrane region in the extracellular domain. This result predicted that alphaCTF is an 80 amino acids fragment. Larger apparent molecular weight of this fragment on Western blotting is probably due to O-linked glycosylation. This result also predicted that N-terminal fragments are released into the culture medium after shedding and that PMA treatment would increase this release. Therefore, we analyzed the culture media by Western blotting and found that there was indeed a CADM1 fragment corresponding in size to NTF after cleavage that produces alphaCTF. As expected, we also found that PMA treatment increased the amount of CADM1 fragments in the culture medium (Fig. 1C).

Taken together, these results suggest that CADM1 shedding produces alphaCTF and a corresponding extracellular fragment, that cleavage occurs in the membrane-proximal region of CADM1 extracellular domain, and that shedding is promoted by PMA.

3.2. CADM1 shedding was detected in an in vitro membrane-fraction incubation assay

CADM1 shedding was previously shown to be inhibited by TAPI-1, a broad-spectrum inhibitor that targets many metalloproteases such as ADAMs and MMPs. Among them, those with transmembrane domains are known to shed a large number of transmembrane substrates.

To obtain further information about CADM1 sheddase, we performed an *in vitro* assay using total cell membrane fraction and focusing on membrane-bound proteases.

To avoid artifacts due to overexpression of CADM1, we prepared total membrane fraction from HEK293 cells, which constitutively express endogenous CADM1. The total membrane fraction prepared by ultracentrifugation was incubated. The level of alphaCTF increased after incubation, whereas that of full-length CADM1 decreased (Fig. 2A). BetaCTF was barely detectable in this preparation. The increase in the 15-kDa band was inhibited by addition of TAPI-1 (Fig. 2A and B), as reported previously by Tanabe et al. [6], who added TAPI-1 to neuronal cells. Serine, cysteine, and aspartic protease inhibitors showed no inhibitory effect on CADM1 shedding (Fig. 2C). Thus, we could reconstitute shedding of CADM1 *in vitro* by incubation of the membrane fraction and could characterize the sensitivity to protease inhibitors using this method. These results indicated that a membrane-associated metalloprotease possesses CADM1 shedding activity.

3.3. CADM1 shedding is mediated by the metalloprotease ADAM10

Many membrane molecules undergo shedding, and ADAM10 and ADAM17 were reported to be two major membrane-associated sheddases. An siRNA approach was employed here to investigate whether ADAM10 and/or ADAM17 cleaved CADM1. The Saos-2 human osteosarcoma cell line, which shows high-level expression of endogenous ADAM10, was used in this assay. The siRNAs used downregulated the mature form of targeted ADAMs as well as the proform (Fig. 3A). Knockdown of ADAM10 expression decreased the amount of alphaCTF, whereas the knockdown of ADAM17 had no effect on the amount of alphaCTF. Furthermore, ADAM10 knockdown abolished PMA-dependent accumulation of alphaCTF (Fig. 3B). These observations indicated that CADM1 is cleaved endogenously by the metalloprotease ADAM10, and PMA-dependent cleavage of CADM1 is also mainly mediated by ADAM10.

3.4. γ-Secretase-like cleavage is abrogated in the presence of γ-secretase inhibitors and in γ-secretase KO cells

Following membrane-proximal cleavage, similar to CADM1 shedding, some membrane proteins undergo a second cleavage mediated by γ-secretase. To determine whether CADM1 is cleaved by γ-secretase, we examined the effects of γ-secretase inhibition on the amounts of cleaved CADM1 fragments after induction of shedding by PMA. COS7-mCADM1 cells were treated with PMA or vehicle alone and then treated with γ-secretase inhibitor (DAPT or L-685,458) or vehicle alone. The amount of alphaCTF increased in

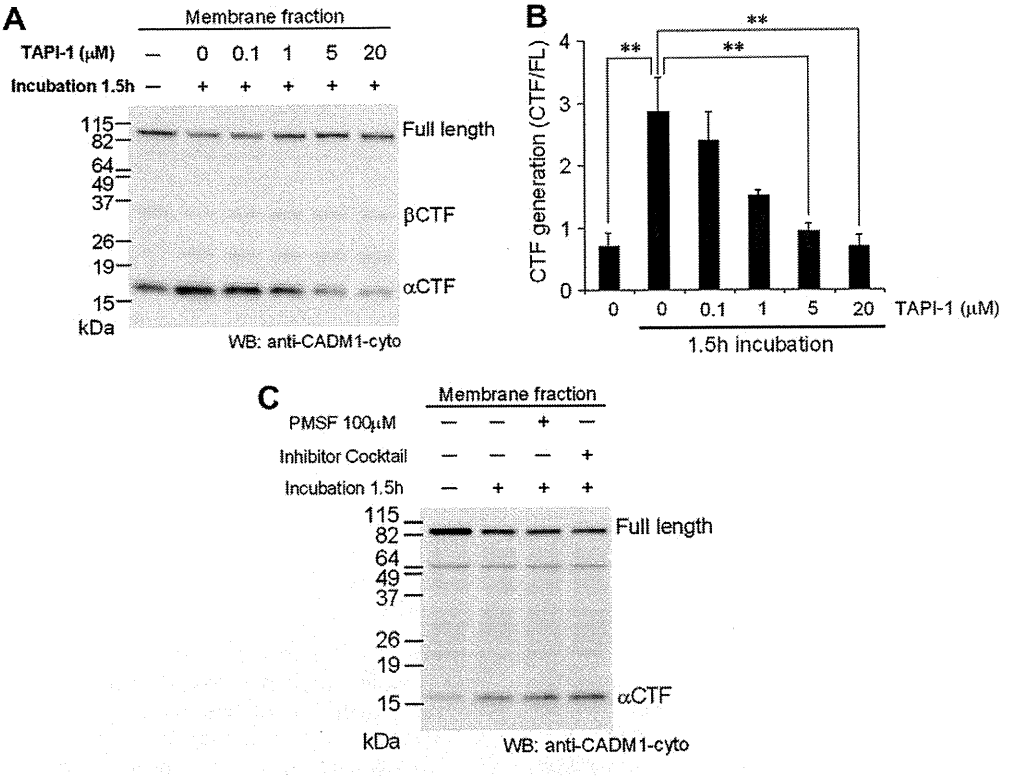

Fig. 2. *In vitro* CADM1 shedding assay. (A–C) Membrane fraction was obtained from HEK293 cells as described in Section 2. The membrane fraction was incubated with the indicated concentration of protease inhibitors and subjected to Western blotting analysis using anti-CADM1-cyto antibody. The results of densitometric analysis of CADM1-CTF generation in (A) are shown in (B). CTF generation was calculated as CTF/full-length ratio by densitometric analysis. Results were obtained from three independent experiments and are expressed as means ± SEM. Data were analyzed by one-way analysis of variance followed by Dunnett's multiple comparison test. **Statistically significant compared with "1.5 h, 0 μM TAPI-1" ($p < 0.01$). The inhibitor cocktail in (C) was from Sigma (P8340).

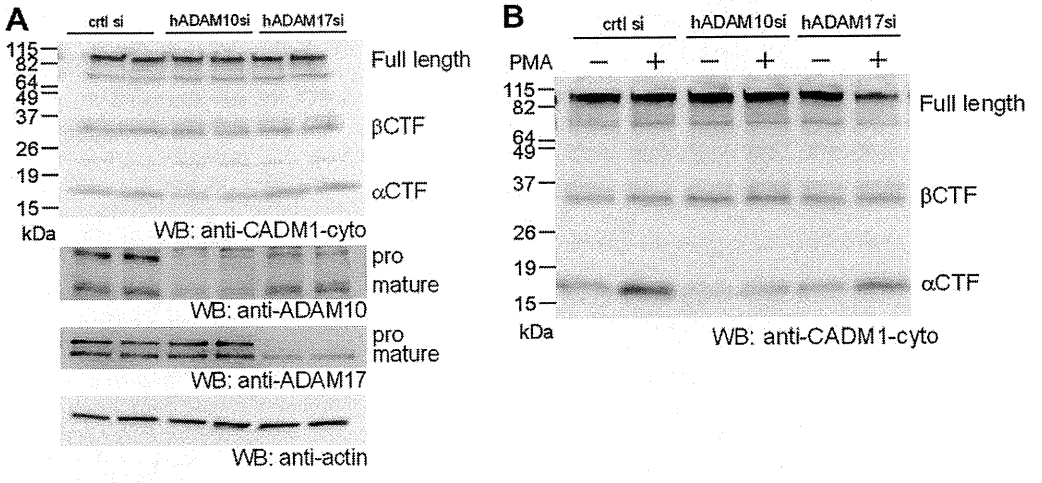

Fig. 3. Knockdown of ADAM10 decreases CADM1-CTF level. (A) Saos-2 cells were transfected with siRNAs against ADAM10 or ADAM17 or with control siRNA. Cells were harvested after 96 h of incubation. Cell lysates were subjected to Western blotting analysis using anti-CADM1-cyto antibody (duplicate results are shown). In (B), cells were treated with 200 ng/mL PMA or vehicle only (DMSO) for 4 h and then harvested.

the presence of γ-secretase inhibitor (Fig. 4A), indicating γ-secretase-dependent degradation of alphaCTF. This finding suggested that alphaCTF was cleaved by γ-secretase into a cytosolic fragment, CICD (CADM1 intracellular domain). With membrane boiling and prolonged exposure, a CADM1-derived band of nearly 6 kDa was detected (Fig. 4A). Membrane boiling contributes to the detection of this 6 kDa fragment, and it is necessary to boil the membrane for the detection of obvious CICD band. The amount of this fragment was decreased with γ-secretase inhibitor treatment, consistent with alphaCTF accumulation (Fig. 4A). γ-Secretase cleaves its substrates within the cell membrane at around three amino acids from the cytosolic end of the transmembrane region of the substrate and generates a fragment with an intact cytoplasmic domain. The theoretical molecular weight of CADM1 cytoplasmic domain is 5.3 kDa. This fragment is the cleavage product of CADM1 generated by γ-secretase. These results suggest that alphaCTF is cleaved by γ-secretase and generates CICD fragments.

We employed another approach to further confirm this possibility. γ-Secretase consists of four proteins, presenilin, nicastrin, Aph-1, and Pen-2, all of which are indispensable for its activity. We used

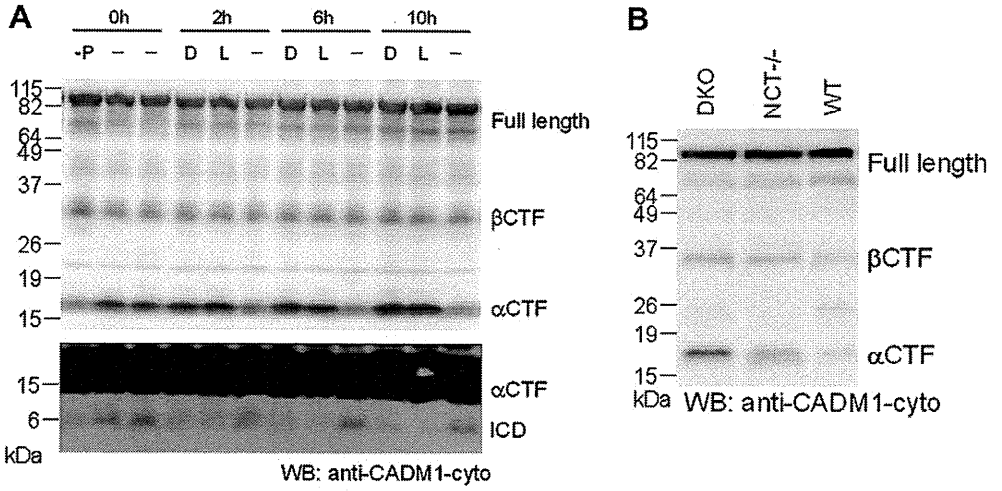

Fig. 4. CADM1-ICD generation is dependent on γ-secretase. (A) COS7-mCADM1 cells were pretreated with 200 ng/mL PMA or vehicle alone (-P: DMSO) for 2 h, and subsequently treated with γ-secretase inhibitors (D: 1 μM DAPT or L: 1 μM L-685,458) or vehicle alone (–: DMSO) and incubated for the indicated times. (B) Cultured cells of two mouse embryonic fibroblast (MEF) cell lines lacking γ-secretase activity and a wild-type MEF cell line were harvested. Cell lysates were analyzed by Western blotting using anti-CADM1-cyto antibody.

two MEF cell lines with no γ-secretase activity, one lacking presenilin-1 and presenilin-2 (PSDKO) and another lacking nicastrin ($NCT^{-/-}$) [16,17]. On Western blotting analysis, the alphaCTF level was increased in γ-secretase KO MEFs but not in wild-type MEFs (Fig. 4B). These results were consistent with those of γ-secretase inhibitor assay, indicating that alphaCTF is processed into CICD by γ-secretase.

4. Discussion

Many previous studies have addressed the various functions of CADM1. Genetic analyses of human cancer suggest that CADM1 has potent tumor-suppressor activity. CADM1 was also shown to suppress tumorigenicity in mouse models, to induce apoptosis, and to suppress cell proliferation *in vitro* [18]. However, the molecular mechanisms underlying these and other functions are largely unknown. In the present study, we focused on membrane protein proteolysis, which may modulate or mediate the functions of such proteins. A previous study indicated that certain CADM1 isoforms are shed due to the action of a ADAM17-like protease [6]. We examined CADM1 proteolysis in more detail, and here we demonstrated the two-step mechanism of CADM1 proteolysis including shedding and RIP with identification of the cleavage site of shedding, sheddase, and subsequent γ-cleavage.

We first demonstrated enhancement of CADM1 shedding by PMA and accumulation of the cleaved extracellular fragment in the medium. A soluble CADM1 isoform was shown to elicit directional neurite extension up a CADM1 concentration gradient [19]. According to the cleavage site determined here, the whole sequence of the soluble isoform was contained within the shed fragment with the exception of two amino acids near the isoform-specific C-terminus. These observations suggest that CADM1 extracellular fragment may also serve as a neurite attractant with a regulated mechanism of secretion. Unexpectedly, although betaCTF was abundant in several cell lines, betaNTF was much less abundant than alphaNTF in the culture medium of the same cells. An as-yet-unknown cellular system may retain and degrade the "extracellular" fragment within the cells.

We developed an *in vitro* shedding assay and demonstrated that CADM1 shedding could occur not only in the intact cell but also in the isolated membrane fraction. This method can be used as a novel *in vitro* assay for ectodomain shedding. To date, *in vitro* shedding assays have mostly been performed by the addition of purified protease to the membrane fraction, which contains the substrate. Our method is closer to physiological conditions because the endogenous localization of a protease and its substrate should be intact. Using this method, we showed here that shedding of CADM1 was directly mediated by a membrane-bound metalloprotease. TAPI-1 was also shown to have an inhibitory effect on CADM1 shedding, consistent with previous findings [6]. Furthermore, the results of siRNA experiments indicated that ADAM10, but not ADAM17, is a potent endogenous sheddase of CADM1. In contrast, previous studies showed that nectin-1 and nectin-4, both of which are adhesion molecules related to CADM1, are cleaved by ADAM10 and ADAM17, respectively [20,21]. ADAM10 is a well-known sheddase that cleaves many other adhesion molecules. Although no consensus cleavage sequence is known for ADAM10, this molecule cleaves its substrate at a site 8–20 amino acids from the transmembrane region in its ectodomain [22]. In the present study, the cleavage site for CADM1 shedding was determined to be nine amino acids from the transmembrane region by MS analysis, indicating that shedding of CADM1 is similar to that of other known cell-surface molecules mediated by ADAM10.

We next showed that CADM1 undergoes γ-secretase-mediated cleavage and generates CADM1-ICD using inhibitors or γ-secretase-deficient cell lines. A previous study indicated that nectin-1α is also cleaved by γ-secretase-like activity to generate ICD [23]. This process is known to involve proteolytic cleavage called RIP, in which removal of the ectodomain by shedding is necessary for the second cleavage catalyzed by γ-secretase [9]. Our data suggested that the substrate of γ-cleavage is the membrane-bound shedding product alphaCTF, consistent with the known mechanism of RIP. Compared with alphaCTF, the amount of CICD fragment is very small, and the difference between the amount of the fragment with and without inhibitor treatment was small. This is probably because of the rapid degradation of CICD, as many other ICD fragments generated by γ-secretase, including Notch ICD, are known to be rapidly degraded in a proteasome-dependent manner [23].

ICD often acts as a signal transducer. Nuclear staining for CADM1 was observed on microscopic analysis using C-terminal GFP-tagged CADM1 or antibody against CADM1 cytosolic domain ([1] and unpublished data). CASK, a protein that binds to CADM1 cytoplasmic domain, is partially localized to the nucleus and interacts with the T-box transcription factor Tbr-1, inducing transcription of genes including NR2b [24]. CADM1-ICD may be transported into the nucleus together with CASK and may modulate

target genes of the Tbr-1-CASK complex. These observations suggest that CADM1 may function in the nucleus as a signal transducer via RIP.

CADM1 is known to act as a tumor suppressor in nude mice, and its expression is reduced in many types of human tumor. ADAM10 is overexpressed in colorectal cancer [25]. The hypermethylation of CADM1 and the reduced expression of CADM1 protein in colorectal cancer have also been reported [26]. ADAM10-mediated shedding may be a mechanism involved in the downregulation of CADM1 in colorectal cancer, which leads to disruption of CADM1-mediated tumor suppression. On the other hand, the functional significance of γ-cleavage is rather complicated. CADM1-ICD has two protein-binding domains, band 4.1 binding domain and PDZ binding domain [1]. These domains are indispensable for the tumor-suppressive functions of CADM1, including tumor suppression in mice, the induction of apoptosis, and the suppression of epithelial-mesenchymal transition [27–29], suggesting the functional significance of the CADM1 cytoplasmic domain.

In conclusion, our data demonstrated that CADM1 cleavage is mediated by ADAM10 and γ-secretase. This mechanism may be important for the downregulation of CADM1 by proteolytic degradation or for tumor-suppressive activity and other functions of CADM1, probably through the activation of CADM1-ICD and reduction of cell–cell adhesion.

Acknowledgments

We thank Dr. Bart De Strooper (Vlaams Instituut voor Biotechnologie) for Presenilin 1/2 double knockout cells and Dr. Philip C. Wong (The Johns Hopkins University) for Nicastrin$^{-/-}$ cells. Y.N. is supported by a JSPS Research Fellowship for Young Scientists.

References

[1] M. Masuda, M. Yageta, H. Fukuhara, et al., The tumor suppressor protein TSLC1 is involved in cell-cell adhesion, J. Biol. Chem. 277 (2002) 31014–31019.
[2] M. Yageta, M. Kuramochi, M. Masuda, et al., Direct association of TSLC1 and DAL-1, two distinct tumor suppressor proteins in lung cancer, Cancer Res. 62 (2002) 5129–5133.
[3] T. Shingai, W. Ikeda, S. Kakunaga, et al., Implications of nectin-like molecule-2/IGSF4/RA175/SgIGSF/TSLC1/SynCAM1 in cell–cell adhesion and transmembrane protein localization in epithelial cells, J. Biol. Chem. 278 (2003) 35421–35427.
[4] H. Fukuhara, M. Masuda, M. Yageta, et al., Association of a lung tumor suppressor TSLC1 with MPP3, a human homologue of Drosophila tumor suppressor Dlg, Dlg. Oncogene 22 (2003) 6160–6165.
[5] Y. Koma, A. Ito, T. Wakayama, et al., Cloning of a soluble isoform of the SgIGSF adhesion molecule that binds the extracellular domain of the membrane-bound isoform, Oncogene 23 (2004) 5687–5692.
[6] Y. Tanabe, T. Kasahara, T. Momoi, et al., Neuronal RA175/SynCAM1 isoforms are processed by tumor necrosis factor-alpha-converting enzyme (TACE)/ADAM17-like proteases, Neurosci. Lett. 444 (2008) 16–21.
[7] A. Ito, T. Jippo, T. Wakayama, et al., SgIGSF: a new mast-cell adhesion molecule used for attachment to fibroblasts and transcriptionally regulated by MITF, Blood 101 (2003) 2601–2608.
[8] A. Ito, M. Hagiyama, T. Mimura, et al., Expression of cell adhesion molecule 1 in malignant pleural mesothelioma as a cause of efficient adhesion and growth on mesothelium, Lab. Invest. 88 (2008) 504–514.
[9] J.O. Ebinu, B.A. Yankner, A RIP tide in neuronal signal transduction, Neuron 34 (2002) 499–502.
[10] I. Okamoto, Y. Kawano, D. Murakami, et al., Proteolytic release of CD44 intracellular domain and its role in the CD44 signaling pathway, J. Cell Biol. 155 (2001) 755–762.
[11] W.T. Kimberly, J.B. Zheng, S.Y. Guenette, et al., The intracellular domain of the beta-amyloid precursor protein is stabilized by Fe65 and translocates to the nucleus in a notch-like manner, J. Biol. Chem. 276 (2001) 40288–40292.
[12] T. Wakayama, H. Koami, H. Ariga, et al., Expression and functional characterization of the adhesion molecule spermatogenic immunoglobulin superfamily in the mouse testis, Biol. Reprod. 68 (2003) 1755–1763.
[13] T. Furuno, A. Ito, Y. Koma, et al., The spermatogenic Ig superfamily/synaptic cell adhesion molecule mast-cell adhesion molecule promotes interaction with nerves, J. Immunol. 174 (2005) 6934–6942.
[14] A. Shevchenko, M. Wilm, O. Vorm, et al., Mass spectrometric sequencing of proteins silver-stained polyacrylamide gels, Anal. Chem. 68 (1996) 850–858.
[15] M. Kikuchi, N. Hatano, S. Yokota, et al., Proteomic analysis of rat liver peroxisome: presence of peroxisome-specific isozyme of Lon protease, J. Biol. Chem. 279 (2004) 421–428.
[16] A. Herreman, L. Serneels, W. Annaert, et al., Total inactivation of gamma-secretase activity in presenilin-deficient embryonic stem cells, Nat. Cell Biol. 2 (2000) 461–462.
[17] T. Li, G. Ma, H. Cai, et al., Nicastrin is required for assembly of presenilin/gamma-secretase complexes to mediate Notch signaling and for processing and trafficking of beta-amyloid precursor protein in mammals, J. Neurosci. 23 (2003) 3272–3277.
[18] Y. Murakami, Involvement of a cell adhesion molecule, TSLC1/IGSF4, in human oncogenesis, Cancer Sci. 96 (2005) 543–552.
[19] M. Hagiyama, N. Ichiyanagi, K.B. Kimura, et al., Expression of a soluble isoform of cell adhesion molecule 1 in the brain and its involvement in directional neurite outgrowth, Am. J. Pathol. 174 (2009) 2278–2289.
[20] J. Kim, C. Lilliehook, A. Dudak, et al., Activity-dependent alpha-cleavage of nectin-1 is mediated by a disintegrin and metalloprotease 10 (ADAM10), J. Biol. Chem. 285 (2010) 22919–22926.
[21] S. Fabre-Lafay, S. Garrido-Urbani, N. Reymond, et al., Nectin-4, a new serological breast cancer marker, is a substrate for tumor necrosis factor-alpha-converting enzyme (TACE)/ADAM-17, J. Biol. Chem. 280 (2005) 19543–19550.
[22] M.S. Rosendahl, S.C. Ko, D.L. Long, et al., Identification and characterization of a pro-tumor necrosis factor-alpha-processing enzyme from the ADAM family of zinc metalloproteases, J. Biol. Chem. 272 (1997) 24588–24593.
[23] D.Y. Kim, L.A. Ingano, D.M. Kovacs, Nectin-1alpha, an immunoglobulin-like receptor involved in the formation of synapses, is a substrate for presenilin/gamma-secretase-like cleavage, J. Biol. Chem. 277 (2002) 49976–49981.
[24] T.F. Wang, C.N. Ding, G.S. Wang, et al., Identification of Tbr-1/CASK complex target genes in neurons, J. Neurochem. 91 (2004) 1483–1492.
[25] T. Knosel, A. Emde, K. Schluns, et al., Immunoprofiles of 11 biomarkers using tissue microarrays identify prognostic subgroups in colorectal cancer, Neoplasia 7 (2005) 741–747.
[26] K. Chen, G. Wang, L. Peng, et al., CADM1/TSLC1 inactivation by promoter hypermethylation is a frequent event in colorectal carcinogenesis and correlates with late stages of the disease, Int. J. Cancer 128 (2011) 266–273.
[27] X. Mao, E. Seidlitz, K. Ghosh, et al., The cytoplasmic domain is critical to the tumor suppressor activity of TSLC1 in non-small cell lung cancer, Cancer Res. 63 (2003) 7979–7985.
[28] X. Mao, E. Seidlitz, R. Truant, et al., Re-expression of TSLC1 in a non-small-cell lung cancer cell line induces apoptosis and inhibits tumor growth, Oncogene 23 (2004) 5632–5642.
[29] M. Masuda, S. Kikuchi, T. Maruyama, et al., Tumor suppressor in lung cancer (TSLC)1 suppresses epithelial cell scattering and tubulogenesis, J. Biol. Chem. 280 (2005) 42164–42171.

Biosci. Biotechnol. Biochem., 75 (2), 396–400, 2011

Communication

Production of Anti-Amyloid β Antibodies in Mice Fed Rice Expressing Amyloid β

Jun NOJIMA,[1] Rika ISHII-KATSUNO,[1] Eugene FUTAI,[1] Noboru SASAGAWA,[1] Yuichiro WATANABE,[1] Taiji YOSHIDA,[2] and Shoichi ISHIURA[1,†]

[1]*Department of Life Science, Graduate School of Arts and Science, The University of Tokyo, 3-8-1 Komaba, Meguro-ku, Tokyo 153-8902, Japan*
[2]*Local Crop Research Team, National Agricultural Research Center for The Tohoku Region, 4 Akahira, Shimo-kuriyagawa, Morioka, Iwate 020-0198, Japan*

Received December 2, 2010; Accepted December 27, 2010; Online Publication, February 7, 2011
[doi:10.1271/bbb.100861]

The main signs of Alzheimer's disease (AD) are cognitive impairment and senile plaques composed of amyloid beta (Aβ) observed in patients' brains. Therefore, therapy for AD focuses on the removal of Aβ. We developed an "edible vaccine" that employs intestinal immunity with little to no side effects. Rice was utilized as an edible vaccine. It expressed GFP-Aβ42. Aβ rice was administered orally to wild-type (WT) mice causing production of anti-Aβ antibodies. Since Aβ rice was mixed with the cholera toxin B subunit (CTB), antibody against the rice seed protein was also produced. Then, mice were caused to develop immune tolerance against the rice seed protein by oral administration of Aβ rice mixed with CTB. The results indicated that only anti-Aβ antibodies were produced.

Key words: Alzheimer's disease; amyloid beta; an edible vaccine; immune tolerance

The main signs of Alzheimer's disease (AD) are cognitive impairment, amyloid beta (Aβ)-containing senile plaques, and neurofibrillary tangles composed of tau observed in a patient's brain.[1)] Aβ is generated by proteolytic processing of the amyloid precursor protein (APP) by β- and γ-secretases. The main species of Aβ are Aβ40 and Aβ42. The longer Aβ42 has a greater propensity to aggregate than the shorter Aβ40.[2)]

In AD model mice, cognitive impairment was improved by inhibiting senile plaque formation by means of antibody production stimulated by vaccination.[3–5)] Vaccination is an antibody therapy that works by timely production of antibodies against the proper antigen. However, in a clinical trial in which Aβ42 peptide was administered to humans, meningoencephalitis was seen as a side effect and the clinical trial was discontinued.[6)] Therefore, a therapy focusing on a mild antigen–antibody reaction is needed. We developed an edible vaccine that induced mild antigen–antibody reaction by oral administration of genetically modified plant-integrated Aβ.

Edible vaccines expressing various antigens have been developed. One benefit of edible vaccines is that they can be maintained at room temperature, whereas peptide vaccines must be preserved at cold temperatures. Furthermore, edible vaccines can eliminate the injection pain associated with traditional vaccines.[7)] They act by stimulating the lymphatic immune system located in the intestines and suppressing the inflammatory Th1 response and enhancing the non-inflammatory Th2 response.

Previously, we expressed GFP-Aβ42 on green pepper leaves. Aβ antibodies were produced when the leaves were administered orally to AD model mice, Tg2576, successfully reducing the Aβ accumulating in their brains.[8,9)] However, new edible vaccines must be developed because green pepper leaves are not easy to digest, and mass production of the antigen is limited.

Rice (cultivar Hayayuki) was chosen as the edible vaccine and, Aβ was expressed as a GFP-fusion protein. GFP-Aβ42 was introduced into the rice by the *Agrobacterium* method (Yoshida, submitted). We performed SDS–PAGE and Western blotting on transgenic rice extracts in urea buffer to detect Aβ expression in the rice. Rice seeds were ground to a fine powder with a IFM-650D Millser (Iwatani International, Tokyo), and total proteins were extracted in urea–SDS buffer (50 mM Tris–HCl, pH 6.8, 8 M urea, 2% SDS, 5% 2-mercaptoethanol, and 20% glycerol) and centrifuged. We used mouse monoclonal antibody 6E10 as the primary antibody to detect Aβ.[9)] Then we quantified the expression of Aβ using synthesized mouse IgG as the protein standard. The Aβ concentration was calculated as 120 μg for 1 g of transgenic rice.

To study antibody production after vaccination and the precise immunological response, subcutaneous and oral immunization of wild-type (WT) B6 mice was performed starting at 6 weeks of age, and was continued for 6 weeks. All the animal experiments followed the guidelines for the regulation of animal experiments of The University of Tokyo. For subcutaneous immunization, each mouse was anesthetized with diethyl ether and injected with 100–200 μL of an emulsion of rice powder dissolved in PBS mixed with Freund's adjuvant (Wako Pure Chemical Industries, Osaka) at several points using a 21-gauge needle. For oral immunization, the mixture of Aβ rice powder and CTB (Sigma-Aldrich, Tokyo) in 5% sucrose was delivered orally by syringe. We examined four groups of WT B6 mice. Five WT mice

† To whom correspondence should be addressed. Tel/Fax: +81-3-5454-6739; E-mail: cishiura@mail.ecc.u-tokyo.ac.jp

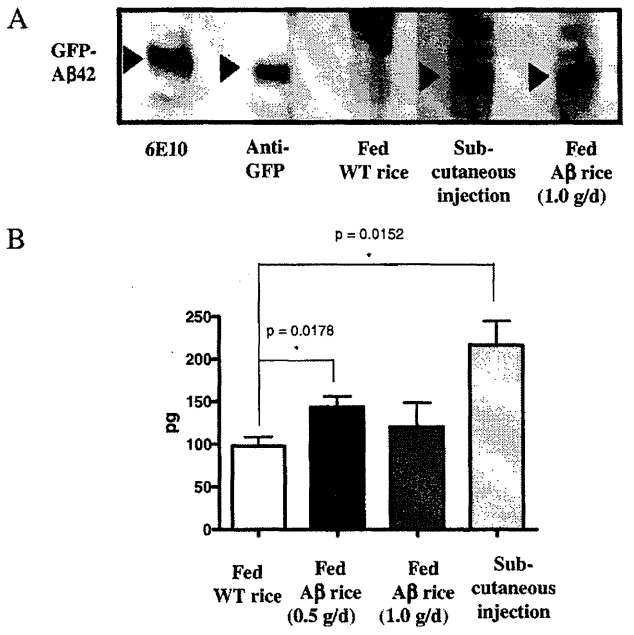

Fig. 1. Detection of Anti-Aβ Antibody in Mice.

A, GFP-Aβ42 was expressed in COS-7 cells and its lysate was separated by SDS–PAGE. Serum was applied to detect anti-Aβ antibody. GFP-Aβ42 was detected in serum from mice fed Aβ rice (1.0 g/d) and injected with the lysate of Aβ rice. For controls, 6E10 and anti-GFP antibody were used. These antibodies also detected GFP-Aβ. B, The amount of anti-Aβ antibody in the serum was calculated ELISA. Serum samples were diluted 100× in this assay. Mean ± SE. $^*p < 0.05$.

vaccinated orally with non-transgenic rice served as negative controls. The rest of the WT mice were immunized with GFP–Aβ42 either subcutaneously (n = 6) or orally (0.5 g/d (n = 5) or 1.0 g/d (n = 4). The mice in the orally administered group received an edible antigen once every week from 6 to 12 weeks of age, and the subcutaneous-injected mice received doses of vaccine biweekly. Two weeks after an Aβ booster given at 12 weeks, whole blood was collected from the heart. GFP–Aβ42 expressed in COS-7 cells was detected in serum from the mice immunized orally (1.0 g/d) and subcutaneously (Fig. 1A). We quantified by ELISA and calculated the amounts of serum anti-Aβ antibody (Fig. 1B).[9] Compared to the WT rice control, the amount of serum anti-Aβ antibody was significantly elevated in the groups receiving GFP–Aβ.

Antibodies against rice seed protein can also be produced by intestinal immunity. That means that food allergy can occur in oral vaccination. We found that an antibody against rice seed protein, possibly prolamin or glutelin, was produced by induction with CTB (Fig. 2A, B). To detect the antibody against rice seed protein in the serum, the serum was diluted 50 times from mice orally administrated Aβ, and was diluted 100 times from mice subcutaneously injected. Rice seed protein-specific IgG responses were measured by ELISA with 20 μg/mL the rice storage protein extracted with 0.01% Triton X-100.[10] Verhasselt *et al.* reported that an antigen can be transferred from lactating mice to their progeny through breast milk.[11] We assumed that the B6 mice acquired immune tolerance through breast milk from lactating mice to which WT rice was administrated orally. In addition, we thought it more efficient to induce immune tolerance through breast-feeding rather than direct administration of WT rice to young mice. Per one lactating mother, six progeny (three male, three female) were prepared. We used two mother mice from the oral administration group and one from the subcutaneously injected group. The WT mice received an edible vaccine orally every week from 6 to 15 weeks of age, and other WT mice received doses of vaccine subcutaneously every 2 weeks. Two weeks after an Aβ booster was given at 15 weeks, whole blood was collected from the heart. The experimental details are schematically shown in Fig. 2C. We found that the amount of antibody against rice proteins tends to be suppressed by oral administration of WT rice to lactating mothers (Fig. 2D, E). The T cell response could be tolerated because the production of the antibody against the rice seed protein is suppressed, but rice seed protein antibody production was not suppressed in mice without pretreatment. Though we tried to quantify the amount of rice protein-induced release of IL-4, -5, and -10 from spleen cells, we were not able to detect these by sandwich ELISA (data not shown).

After inducing immune tolerance by oral administration of WT rice to lactating mice, we investigated the production of anti-Aβ antibodies. We found that they were significantly elevated in the group receiving Aβ rice orally as compared to the group given WT rice (Fig. 3A). Next we investigated which sites of Aβ42 peptide were recognized. Using Aβ1-16 (Peptide Institute, Osaka, Japan), Aβ11-28 (Immuno-Biological Laboratories, Takasaki, Japan) and Aβ25-35 peptide (Peptide Institute), epitope mapping of anti-Aβ antibody was done by ELISA (Fig. 3B). The results suggested that the antibodies produced by oral administration or subcutaneous injection recognized a wide variety of Aβ epitopes, because no differences were observed among Aβ1-16, Aβ11-28, Aβ25-35, and Aβ1-42.

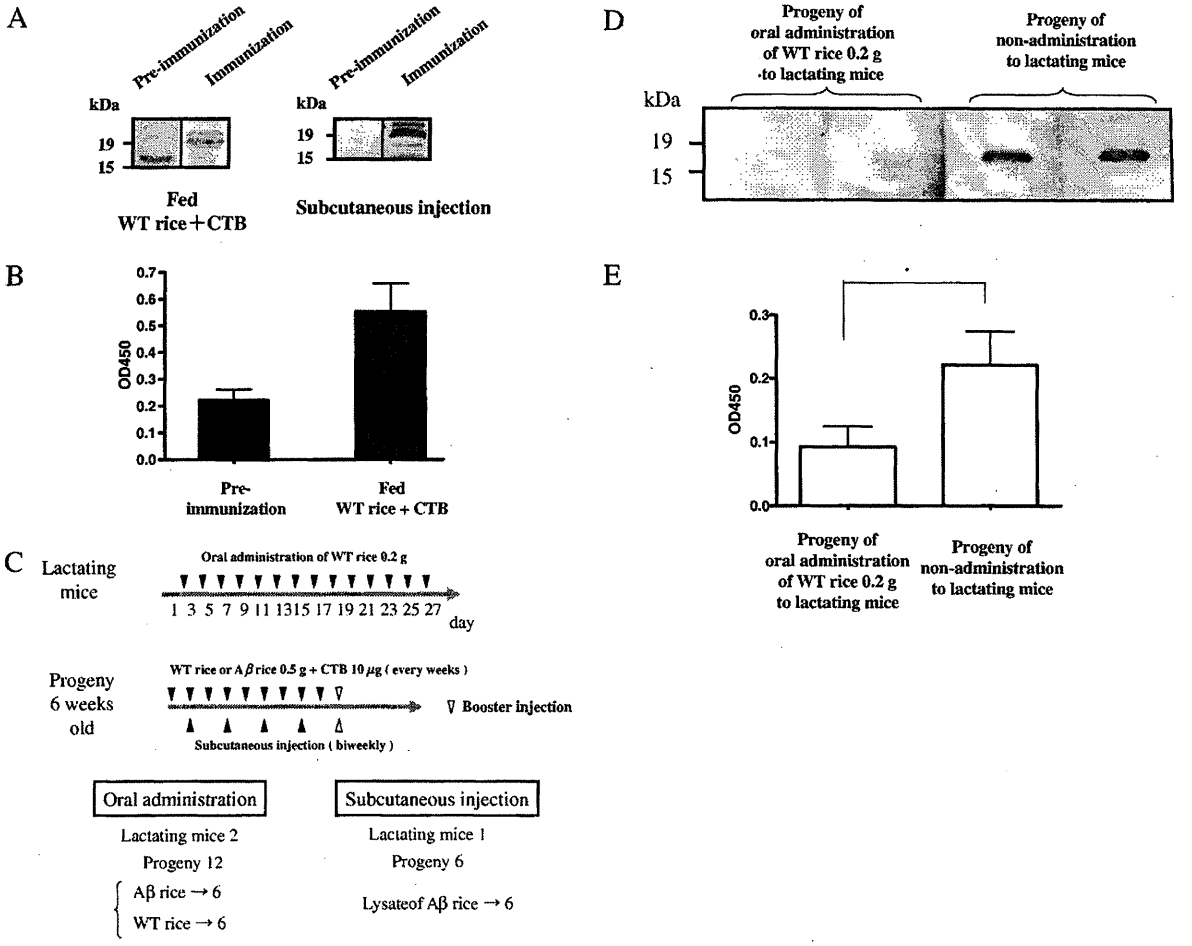

Fig. 2. Production of Anti-Rice Storage Protein Antibodies in Mice.

A, The difference in the production of the antibody against the rice seed protein before and after immunization was investigated SDS–PAGE. After immunization, anti-rice seed proteins were observed in both oral (left) and subcutaneous injection (right). B, The amount of the antibody against the whole rice seed protein was calculated ELISA. C, Experimental protocol. Lactating mothers were orally administrated wild rice (0.2 g) every other day from delivery until weaning. D, Rice extract in urea–SDS buffer was applied to SDS gels, and the various sera was used to detect anti-rice seed protein antibody. The rice storage protein (15–19 kDa) was not detected in the serum from progeny of oral administration of WT rice to lactating mice (left). High antibody production was observed in the mice without prior administration of rice (right). Serum samples were diluted to 50× in this assay. E, Amount of antibody against rice whole protein. The value of the newly developed anti-rice protein antibody due to Aβ-rice is shown. Production against the rice protein was suppressed in mice whose mothers were orally administrated rice at the lactating stage. Mean ± SE. $^*p < 0.05$.

To check the safety of the edible vaccine, we examined the isotype of anti-seed protein antibody in the serum and looked for inflammatory reactions in mice vaccinated orally and subcutaneously. IgG1 is known to be the non-inflammatory Th2 isotype IgG, and IgG2a is the inflammatory Th1 isotype IgG. If the ratio of IgG1/IgG2a exceeds 1, the humoral immune responses of the non-inflammatory Th2 act dominantly. Therefore, to quantify rice seed protein specific immunoglobulin subclasses produced by intestinal immunity (orally administration) and systemic immunity (subcutaneous injection), ELISA with IgG1 and IgG2a was done. The ratio of IgG1 to IgG2a (IgG1/IgG2a) was calculated. In all the groups, the ratio of IgG1/IgG2a exceeded 1, suggesting that feeding of Aβ rice induced the Th2 response (data not shown).

The number of patients with AD continues to increase and this is predicted to become a major problem, but no effective therapy exists.[12,13] According to the amyloid hypothesis, AD is triggered by an accumulation of Aβ, and peculiar pathogenic changes, such as neurologic deficit, are seen in AD brains.[1] Therefore, the focus for therapy of AD is to suppress the production of Aβ or to inhibit the deposition of Aβ in the brain.[14] To remove Aβ from the brain, antibody therapy *via* injection of Aβ into the body was performed at the beginning of 2000, but meningoencephalitis appeared as a side effect.[6] Therefore, the conclusion was drawn that the therapy needs a mild antigen–antibody reaction with a non-inflammatory response toward Th2.

Hence we started a study of edible vaccines.[8] Because edible vaccines work through intestinal immunity, which induces the Th2 reaction and produces antibodies, it was thought to have few side effects. We expressed GFP-Aβ42 in green pepper leaves with *Tobamovirus*, and these lysates mixed with CTB were orally administrated to AD model mice, Tg2576. We succeeded in producing anti-Aβ antibodies and decreased Aβ in the mouse brains. We also observed that the edible vaccine induced a noninflammatory response toward Th2.[9]

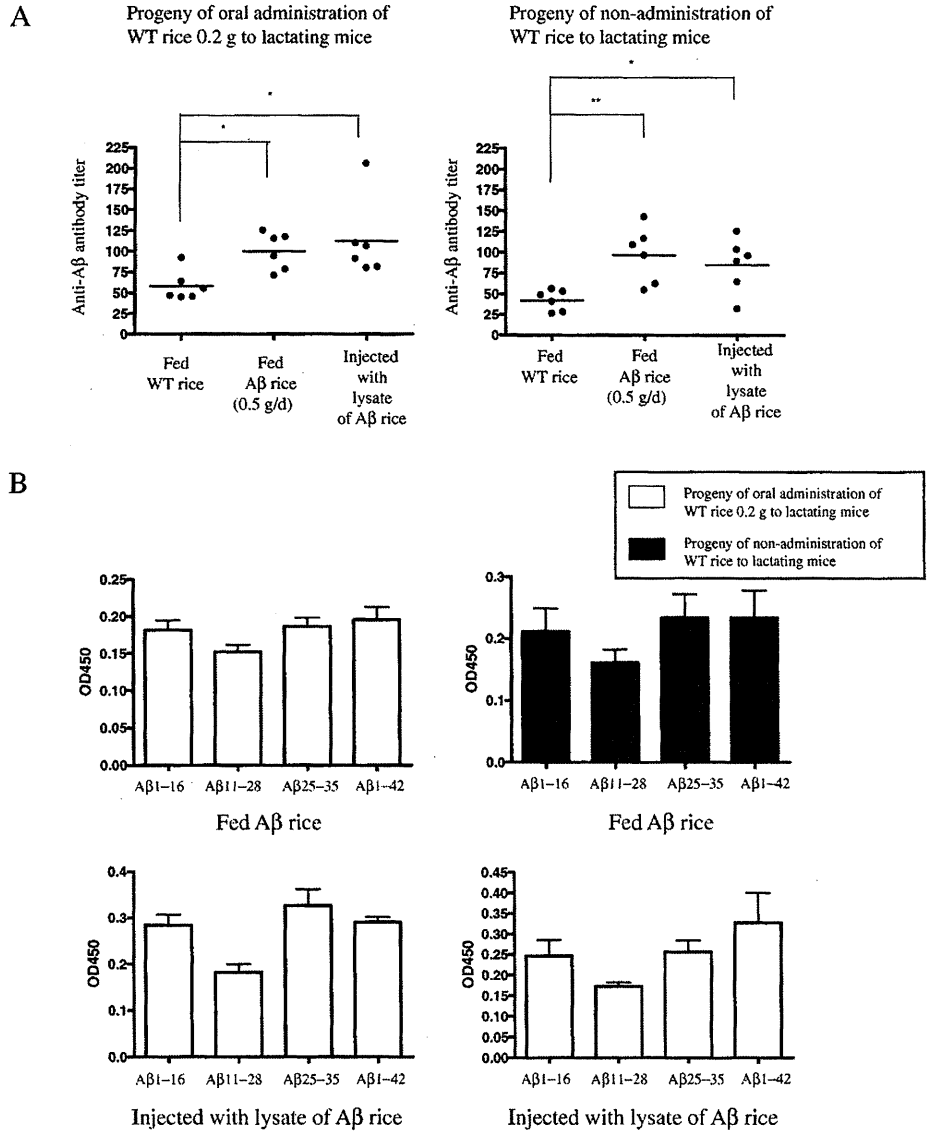

Fig. 3. Detection of Anti-Aβ Antibody in Mice and Epitope Mapping.
A, The Aβ-antibody titers of the mice are shown ($*p < 0.05$, $**p < 0.01$). B, The epitope mapping of Aβ. The peptides of Aβ1-16, Aβ11-28, and Aβ25-35 were used as antigens. Sera from mice fed Aβ rice or injected with the lysate of Aβ rice were used in the assay.

We investigated to determine whether the antibody against Aβ would be produced by oral administration of Aβ rice to B6 mice, as in the case of green pepper leaves. Compared to the group with oral administration of WT rice, the amount of anti-Aβ antibody increased significantly in the group subjected to oral administration of Aβ rice and in that receiving subcutaneous injections (Fig. 1A, B), but the antibody titer against Aβ did not increase greatly. We found that the anti-Aβ antibody titer was inversely correlated with the level of soluble intracerebral Aβ42 in Tg2576 mice in the green pepper experiment.[9] The frequency of immunization was different in this rice experiment, and the possibility exists that the effect of CTB attenuates it, because the amounts of proteins in rice are larger than in green pepper leaves. In the case of transgenic rice expressing *Chlamydophila psittaci* (*Cp. Psittaci*) antigen (MOMP)-fused LTB, mice were fed large amounts of rice in order to produce an antibody against MOMP.[15] Additionally, immunizing the AD model mice for a long time is important to decrease senile plaques, so one can remove Aβ in Tg2576 mice even if an antibody is produced in modest amounts.[16]

Because we administered CTB orally, antibody against rice seed protein was produced. However, as for humans, some believe that one can suppress antibody production due to immune tolerance against rice seed proteins by eating rice frequently. Since it has been reported to induce immune tolerance through lactation,[11] we tried to produce an antibody against Aβ by suppressing antibody production against rice seed proteins by administering lactating mice WT rice. Even if humans use an edible vaccine with CTB, the antibody against the rice seed proteins may be suppressed. However, because IgE rather than IgG is the main immunoglobulin produced in food allergy, the production of IgE must also be also investigated in the future. Although the antibody against CTB was reportedly

produced by the rice that expressed CTB, the antibody against the rice seed protein was not produced.[10] Therefore, rice expressing Aβ with CTB might not produce antibody against rice seed protein, when immune tolerance is induced.

We performed epitope mapping and found that various antibodies were produced. The antibodies recognizing the N-terminus, such as Aβ1-6, are efficient at inhibiting the formation of senile plaques, and the antibody used in the clinical trials has tandem repeats recognizing the N-terminus.[17–19] This food vaccine must improve a DNA construct to produce the antibody recognizing the N-terminus effectively and to fuse oral adjuvants such as CTB, instead of GFP for clinical use. Furthermore, we examined the T-cell response by calculating IgG1/IgG2a. In our system, intestinal immunity is thought to act dominantly on the Th2 immune response.

In this study, we were able to confirm the possibility of a vaccine treatment for AD. Rice is valuable as an edible vaccine because the effect of the vaccine reportedly is not lost even if the rice is preserved at room temperature for more than 1 year.[10] However, we must use AD model mice in future studies and examine the utility of the vaccine in AD therapy.

References

1) Hardy J and Selkoe DJ, *Science*, **297**, 353–356 (2002).
2) Tanahashi H and Tabira T, *Neurosci. Lett.*, **428**, 103–108 (2007).
3) Schenk D, Barbour R, Dunn W, Gordon G, Grajeda H, Guido T, Hu K, Huang J, Johnson-Wood K, Khan K, Kholodenko D, Lee M, Liao Z, Lieberburg I, Motter R, Mutter L, Soriano F, Shopp G, Vasquez N, Vandevert C, Walker S, Wogulis M, Yednock T, Games D, and Seubert P, *Nature*, **400**, 173–177 (1999).
4) Janus C, Pearson J, McLaurin J, Mathews PM, Jiang Y, Schmidt SD, Chishti MA, Horne P, Heslin D, French J, Mount HT, Nixon RA, Mercken M, Bergeron C, Fraser PE, St George-Hyslop P, and Westaway DA, *Nature*, **408**, 979–982 (2000).
5) Morgan D, Diamond DM, Gottschall PE, Ugen KE, Dickey C, Hardy J, Duff K, Jantzen P, DiCarlo G, Wilcock D, Connor K, Hatcher J, Hope C, Gordon M, and Arendash GM, *Nature*, **408**, 982–985 (2000).
6) Orgogozo JM, Gilman S, Dartigues JF, Laurent B, Puel M, Kirby LC, Jouanny P, Dubois B, Eisner L, Flitman S, Michel BF, Boada M, Frank A, and Hock C, *Neurology*, **61**, 46–54 (2003).
7) Matsumoto Y, Suzuki S, Nozoye T, Matsumoto Y, Suzuki S, Nozoye T, Yamakawa T, Takashima Y, Arakawa T, Tsuji N, Takaiwa F, and Hayashi Y, *Transgenic Res.*, **2**, 185–192 (2009).
8) Szabó B, Hori K, Nakajima A, Sasagawa N, Watanabe Y, and Ishiura S, *Assay Drug Dev. Technol.*, **18**, 383–388 (2004).
9) Ishii-Katsuno R, Nakajima A, Katsuno T, Nojima J, Futai E, Sasagawa N, Yoshida T, Watanabe Y, and Ishiura S, *Biochem. Biophys. Res. Commun.*, **399**, 593–599 (2010).
10) Nochi T, Takagi H, Yuki Y, Yang L, Masumura T, Mejima M, Nakanishi U, Matsumura A, Uozumi A, Hiroi T, Morita S, Tanaka K, Takaiwa F, and Kiyono H, *Proc. Natl. Acad. Sci. USA*, **104**, 10986–10991 (2007).
11) Verhasselt V, Milcent V, Cazareth J, Kanda A, Fleury S, Dombrowicz D, Glaichenhaus N, and Julia V, *Nat. Med.*, **14**, 170–175 (2008).
12) Ziegler-Graham K, Brookmeyer R, Johnson E, and Arrighi HM, *Alzheimer's Dement.*, **4**, 316–323 (2008).
13) Brookmeyer R, Johonson E, Ziegler-Graham K, and Arrighi HM, *Alzheimer's Dement.*, **3**, 186–191 (2007).
14) Tabira T, *Tohoku J. Exp. Med.*, **220**, 95–106 (2010).
15) Zhang X, Yuan Z, Duan Q, Zhu H, Yu H, and Wang Q, *Vaccine*, **27**, 1596–1600 (2009).
16) Sigurdsson EM, Knudsen E, Asuni A, Fitzer-Attas C, Sage D, Quartermain D, Goni F, Frangione B, and Wisniewski T, *J. Neurosci.*, **24**, 6277–6282 (2004).
17) Bard F, Barbour R, Cannon C, Carretto R, Fox M, Games D, Guido T, Hoenow K, Hu K, Johnson-Wood K, Khan K, Kholodenko D, Lee C, Lee M, Motter R, Nguyen M, Reed A, Schenk D, Tang P, Vasquez N, Seubert P, and Yednock T, *Proc. Natl. Acad. Sci. USA*, **100**, 2023–2028 (2003).
18) Kim HD, Maxwell JA, Kong FK, Tang DC, and Fukuchi K, *Biochem. Biophys. Res. Commun.*, **336**, 84–92 (2005).
19) Lemere CA and Masliah E, *Nat. Rev. Neurol.*, **6**, 108–119 (2010).

International Journal of Biological Sciences
2011; 7(3):301-307

Short Research Communication

Transgenic Rice Expressing Amyloid β-peptide for Oral Immunization

Taiji Yoshida[1,✉], Eiichi Kimura[1], Setsuo Koike[1], Jun Nojima[2], Eugene Futai[2], Noboru Sasagawa[2], Yuichiro Watanabe[2], and Shoichi Ishiura[2]

1. National Agricultural Research Center for Tohoku Region, National Agriculture and Food Research Organization, Iwate, Japan
2. Department of Life Sciences, Graduate School of Arts and Sciences, The University of Tokyo, Tokyo, Japan

✉ Corresponding author: T. Yoshida, National Agricultural Research Center for Tohoku Region, National Agriculture and Food Research Organization, 4 Akahira, Shimo-kuriyagawa, Morioka, Iwate 020-0198, Japan. Tel: +81 19 643 3528; Fax: +81 19 643 3698; E-mail address: yoshidat@affrc.go.jp

Received: 2010.12.11; Accepted: 2011.03.22; Published: 2011.03.25

Abstract

Various vaccine therapies for Alzheimer's disease (AD) have been investigated. Here we report transgenic rice expressing amyloid β-peptide (Aβ). The Aβ42 gene fused with a green fluorescent protein gene was introduced into rice using the *Agrobacterium* method. When transgenic brown rice expressing Aβ was orally administered to mice, serum anti-Aβ antibody titers were elevated. The same results were observed when mice were fed boiled, transgenic brown rice. The results indicate that an edible vaccine against AD using rice may be feasible. A vaccine derived from rice would be far cheaper than existing medical vaccines.

Key words: Alzheimer's disease, amyloid β-peptide, edible vaccine, Oryza sativa, brown rice

Introduction

Alzheimer's disease (AD) causes cognitive impairment and while symptomatic therapies such as donepezil hydrochloride are available, no existing therapeutic medication offers complete recovery from AD. The development of new AD therapies would lessen the social and economic burden of the disease.

The onset of AD is thought to be due to amyloid β-peptide (Aβ) deposition in the cerebral cortex [1,2]. As Aβ is a protein, vaccines for AD are potential means of therapy or prevention [3-5]. In trials using mouse models of AD, injection with Aβ as an antigen reduced the level of Aβ accumulation in the brain notably, reduced memory defects and improved behavioral disorders [6,7]. A phase I clinical trial of vaccine therapy by intramuscular injection of Aβ was completed without problems but the phase II clinical trial was terminated because some patients developed meningoencephalitis [8]. In a 6-year follow-up of patients in the trial of AD immunization [9], cortical Aβ loads were lower in immunized patients compared to the control group. Patients with higher antibody responses had more extensive Aβ removal. However, this study did not find survival or time to severe dementia improved in immunized patients versus the control group.

A vaccine therapy with no side effects is needed. Oral or other mucosal vaccinations appear to have fewer side effects than vaccines administered by injection [10,11]. A potential method of oral vaccination is to express a target protein in an edible plant. Increased serum anti-Aβ antibody titer and suppressed Aβ deposition in the brain were observed when green pepper or potato containing Aβ was fed to a mouse model of AD [11,12,13,14]. Edible vaccine might also be produced in genetically modified food plants such as rice or soybeans that accumulate Aβ in seeds. Ce-

real seeds are better suited for edible vaccines than fruit or vegetables as many have high protein content and can be stored for long periods at room temperature.

In the present study, we introduced the Aβ gene conjugated with green fluorescent protein (GFP) into rice, and orally administered modified rice to mice in order to investigate the effects of Aβ on serum anti-Aβ antibody titer.

Materials and Methods

Plant materials

Oryza sativa L. cultivar Hayayuki (Japonica rice in Japan) was used in this study. Mature seeds (brown rice) were sterilized in 70% ethanol for 10 s and 1% sodium hypochlorite for 15 min, and rinsed in sterile distilled water. Seeds were placed on N6D medium [15,16] for callus formation. Cultures were incubated at 25°C under a 16-h photoperiod using cool-white fluorescent light at 40 μmol/m²/s. Calli were isolated from seed scutella 10-30 days later, and used for Aβ gene induction.

Plasmid construction

The nucleoside sequence coding Aβ42 was amplified by PCR using primers Aβ-5′-XhoI (5′-GAAGTCTCGAGTGATGCAGAAT-3′) and Aβ-3′-HindIII (5′-GAACGAAGCTTTTACGCTATGA CA-3′). The gene for the APP695 protein was used as a template. The product was digested with XhoI and HindIII, and inserted into pEGFP-C2 (Clontech) at restriction sites resulting in pEGFP-Aβ-C2.

The nucleoside sequence coding sGFP(S65T) [17] was amplified by PCR using primers sGFP-5′-AgeI (5′-ATACCGGTCGCCACCATGGTGAGCAAGGGC GAG-3′) and sGFP-3′-BglII (5′-TCAGATCTGAGT CCGGCCGGACTTGTACAGCTCGTCCAA-3′). The product was digested with AgeI and BglII, and ligated to the pEGFP-Aβ-C2 at the restriction sites to produce psGFP-Aβ-C2. The GFP-Aβ fused gene was produced by amplifying psGFP-Aβ-C2 by PCR using primers sGFP-5′-XbaI (5′-TTTCTAGAATGGTGAGCAAGG GCGAGGAG-3′) and Aβ-3′-SacII (5′-TTGAGCT CGACTGCAGAATTCGAAGCTT-3′), followed by digestion with XbaI and SacII.

The binary vector pIG121-Hm [18] was digested with XbaI and SacII to remove the Intron-Gus gene. The GFP-Aβ fused gene was then ligated to pIG121-Hm to produce pIG121-Hm (sGFP+Aβ).

The binary vector pIG121-Hm (sGFP+Aβ) was electroporated into *Agrobacterium tumefaciens* strain EHA101 using an *Escherichia coli* pulser (Bio-Rad). Transformants EHA101 (pIG121-Hm (sGFP+Aβ)) were selected on LB medium containing 50 mg/L kanamycin, 50 mg/L hygromycin B and 1.2% Bacto-agar.

Transformation

EHA101 (pIG121-Hm (sGFP+Aβ)) was grown overnight on LB medium with 50 mg/L kanamycin, 50 mg/L hygromycin, and 1.2 % Bacto-agar at 25°C. Bacteria were suspended in AAM medium [19]. Rice calli were immersed in AAM medium containing the bacteria for 15 min.

Calli were transferred to N6D medium, modified to pH 5.2, containing 100 μM acetosyringone, and incubated in the dark at 22°C for 3 days. After co-cultivation, calli were washed with the medium (N6 salts, N6 vitamins, 2 mg/L 2,4-D, 30 g/L sucrose, 400 mg/L carbenicillin, pH 5.8).

Washed calli were cultured on selective media (N6D medium with 50 mg/L hygromycin B and 400 mg/L carbenicillin) at 25°C under a 16-h photoperiod. White or yellow calli were transferred every 10 days to the same medium.

Calli were transferred to plant regeneration medium [20] modified with 100 mg/L carbenicillin. Cultures were incubated at 25°C under a 16-h photoperiod. Calli with green spots or plantlets were transferred every 5-10 days, until the plantlets grew to more than 1 cm in height. Plantlets were transferred into hormone-free MS medium, and fully grown plantlets were planted in soil.

Southern blot analysis

Extracted leaf DNA was digested with XbaI. Electrophoresis was performed on 1.0% agarose gels, and DNAs were blotted onto a Hybond-N+ membrane (GE Healthcare) and were subjected to Southern hybridization. GFP sequence containing the whole coding region was used as a probe. Probe labeling and southern hybridization procedures were performed using the AlkPhos direct labeling and detection system with CDP-Star (GE Healthcare).

Quantification of expression levels in seeds

Frozen seeds were crushed. Total protein in one seed (approximately 20 mg) was extracted for 1 h with 400 μL protein extraction buffer (20 mM Tris-HCl (pH 6.5), 8 M urea, 5% 2-mercaptoethanol, 20% glycerol, 4% SDS), and was centrifuged for 10 min at 20,000 × *g*. Three microliters of each supernatant was applied to Tris-Tricine SDS-PAGE (12% T, 3% C) together with Aβ (human, 1-42) (Peptide Institute) as standards, and the separated protein were transferred to a Hybond-P PVDF membrane (GE Healthcare). The membrane was first incubated in blocking buffer (5% skim milk, T-PBS), and treated with anti-Aβ antibody 6E10 (Sig-

net). The GFP-Aβ fusion protein bound to the membrane was detected using the HRP-conjugated secondary antibody (GE Healthcare) and the ECL plus Western blotting detection system (GE Healthcare).

Mouse immunization

The quantity of brown rice administered to each mouse was adjusted to deliver 10 μg of Aβ. Crushed brown rice was mixed with cholera toxin B (CTB, List Biological Laboratories) (5 μg per mouse) in PBS. C57BL/6J mice (Charles River) were divided into three groups (eight mice per group) and were orally fed with a feeding needle (non-transgenic brown rice, Aβ-containing brown rice (Aβ rice), or boiled Aβ rice). Mice received doses of rice once a week from 8 to 11 weeks of age. As a booster, 0.5 μg of Aβ mixed with Freund's incomplete adjuvant was injected subcutaneously into all mice at 14 weeks of age. Blood serum was collected at 8, 12, 14, and 16 weeks of age. Mice were housed at 25°C with a 12-h light/dark cycle. All animal procedures were approved by the Animal Care and Use Committee of the National Agricultural Research Center for the Tohoku Region.

Quantification of the anti-Aβ antibody titer with ELISA

Micro plate wells were coated with Aβ42 dissolved in 0.15 M ammonium. After washing with PBS-T, wells were blocked with blocking buffer (3% skim milk, PBS), and were washed. Blood serum samples were diluted 10-50 times. Anti-Aβ antibody 6E10 (1 mg/mL) was diluted 10,000-160,000 times as a positive control. Each sample was applied to a well and incubated at 37°C for 1 h. After washing, each well was blocked at room temperature for 30 min with 3% skim milk and was washed again. Wells were incubated with HRP-conjugated secondary antibody at 37°C for 1 h and were washed. Wells were incubated with a TMB kit (Pierce) at room temperature in the dark. The reaction was stopped with 2 M sulfuric acid. Absorbance at 450 nm was measured with a spectrophotometer (Infinite F300, Tecan), and antibody titers were calculated (0.1 μg/mL 6E10 = 100 units/mL antibody titer).

Detection of the anti-Aβ antibody production by Western blot analysis

Aβ (240 ng) was applied to l2% polyacrylamide gels containing 0.1% SDS; separated proteins were transferred to a Hybond-P PVDF membrane. The membrane was first incubated in blocking buffer (ECL Advance blocking agent, GE Healthcare), and treated with serum samples (10 times dilution). Anti-Aβ production was detected by HRP-conjugated secondary antibody and the ECL advance Western blotting detection kit (GE Healthcare).

Results and Discussion

Initially, the luminescence of transgenic rice expressing the EGFP-Aβ fusion gene was weak. The sGFP(S65T) gene is designed for plant use and gives brighter light in the plant than the original GFP [17]. We therefore expressed sGFP instead of EGFP in rice, and the resulting transgenic rice seeds exhibited stronger luminescence with many fluorescent spots (Fig. 1A, B). Fluorescence was localized mainly in the aleurone layer of brown rice (Fig. 1C). Polished rice had a little fluorescence (Fig. 1D).

These results show that Aβ accumulates in aleurone layer, and if brown rice is polished, a proportion of Aβ is removed from the rice. Most rice eaten in Japan is polished, and brown (non-polished) rice must be eaten for AD vaccination to succeed.

The presence of the Aβ-GFP gene in the leaves of primary transgenic rice plants (R_0 rice plants) was investigated by PCR analysis using primers sGFP-5'-XbaI and Aβ-3'-SacII (data not shown). In samples where PCR analysis indicated the presence of the Aβ-GFP gene, Southern blot analysis was used to confirm transformation in individual plants (Fig. 2). The Aβ-GFP gene was introduced into R_0 plants except line No. 32. The positive PCR result in the Line No. 32 plant may have been due to residual *Agrobacterium* in plant tissue.

Western blotting was used to investigate the accumulation of the Aβ-GFP fusion protein in Aβ transgenic rice (Fig. 3). The signal intensity of the band was compared against the signal intensity of Aβ42 as a control, and differences were observed among lines. The highest concentration, 8 μg of Aβ in a single grain of brown rice (400 μg/g brown rice) was found in samples from line 29, compared with 18-50 μg Aβ [13] and 77 μg Aβ [14] per gram of soluble protein found in potato in previous studies.

Immunogenicity of Aβ rice was assessed by feeding brown Aβ rice to C57BL/6J mice, from 8 to 11 weeks of age, and assessing serum anti-Aβ antibody titer by ELISA (Fig. 4). At 12 weeks age, we observed a significant increase in serum anti-Aβ antibody titer in mice fed boiled Aβ rice; the increase was not significant in mice fed uncooked Aβ rice. Anti-Aβ antibody was also detected by Western blot analysis in mice fed Aβ rice (Fig. 4B). No increase of anti-Aβ antibody titer was detected in mice at 14 weeks of age, three weeks after the last oral administration (Fig. 4C); but the anti-Aβ antibody titer significantly increased again at 16 weeks of age, after a subcutaneous booster injection (Fig. 4D).